Institut de Physique
Université de Neuchâtel

Croissance épitaxiale par jets moléculaires de couches minces de $La_{2-x}Sr_xCuO_4$ et étude de leurs propriétés structurales et supraconductrices en fonction du dopage x

THESE

présentée à la Faculté des Sciences
de l'Université de Neuchâtel
pour l'obtention du grade de docteur ès sciences

par
Yvan Jaccard
physicien diplômé
de l'Université de Neuchâtel

Neuchâtel, septembre 1996.

IMPRIMATUR POUR LA THÈSE

Croissance épitaxiale par jets moléculaires de couches minces de $La_{2-x}Sr_xCuO_4$ et étude de leurs propriétés structurales et supraconductrices en fonction du dopage x

de M. Yvan Jaccard

UNIVERSITÉ DE NEUCHÂTEL

FACULTÉ DES SCIENCES

La Faculté des sciences de l'Université de Neuchâtel sur le rapport des membres du jury,

Messieurs P. Martinoli, H-. Beck, O Fischer (Genève), T. Schneider (Zürich) et J.-P. Loquet (Rüschlikon)

autorise l'impression de la présente thèse.

Neuchâtel, le 30 septembre 1996

Le doyen:

R. Dändliker

Résumé

Le fruit de ce travail provient d'une collaboration entre les Universités de Genève et de Neuchâtel et du laboratoire de recherche d'IBM à Zurich.

Nous avons étudié certaines propriétés physiques en fonction de la concentration x de couches minces de $La_{2-x}Sr_xCuO_4$ crues sur $SrTiO_3$ par un système de croissance épitaxiale par jets moléculaires (MBE).

Les propriétés normales de ces couches ont été étudiées au travers de mesures résistives et d'effet Hall. Pour une température donnée, ces deux grandeurs montrent une décroissance monotone avec la concentration x indiquant une croissance monotone des porteurs de charge avec cette même concentration. Cependant, la résistivité montre, indépendamment du dopage, une valeur absolue de $20 - 30\%$ plus grande que celle de cristaux. Une telle différence fut expliquée par le mismatch entre le réseau du substrat et celui du '214'. La maille de celui-ci subit une élongation de son plan ab mis en évidence par la contraction du paramètre perpendiculaire c.

Les propriétés supraconductrices ont été mesurées par une technique inductive. Une telle mesure nous donne des informations sur la profondeur de pénétration et l'énergie d'activation du mouvement des vortex de ces couches.
Comme la mesure inductive est une mesure très sensible au voisinage de la température critique, nous avons cherché à connaître le comportement critique de la profondeur de pénétration. L'utilisation de la théorie phénoménologique de Ginzburg-Landau, en exigeant plus qu'un traitement de type champ moyen, nous permet d'extraire cette grandeur. La combinaison de cette théorie avec celle d'un effet de taille nous a montré que le comportement critique de la profondeur de pénétration appartient à la classe d'universalité du modèle 3D-XY. Le comportement non-monotone de cette grandeur avec la concentration est une simple conséquence de la dépendance de la température critique avec cette même concentration.
Les mesures en champ magnétique ont permis d'extraire une énergie d'activation du mouvement des vortex. Comme pour les autres grandeurs déterminées, cette énergie montre un comportement non-monotone avec le dopage. La dépendance en champ magnétique de cette énergie a premièrement, confirmé la non-monotonie de la profondeur de pénétration avec la concentration, comme observé directement par la mesure en température de la profondeur de pénétration, et deuxièmement, montré le caractère quasi-bidimensionnel du réseau de vortex dans ces couches indépendamment de la concentration.

Note: Ce fascicule correspond à une forme réduite de la thèse.

Un texte complet de cette thèse a été déposé à la bibliothèque principale de l'Université de Neuchâtel.

Liste des publications majeures

1. Y. Jaccard, A. Cretton, E. J. Williams, J.-P. Locquet, E. Mächler, C. Gerber, T. Schneider, Ø. Fischer and P. Martinoli.
   Characterisation of MBE-grown ultrathin films in the $La_{2-x}Sr_xCuO_{4+\delta}$ system.
   Proc. of SPIE Conf. on Oxide Superconductors Physics and Nano-Engineering, Los Angeles, 26-28 January 1994, SPIE **2158**, 200.

2. E. J. Williams, A. Cretton, Y. Jaccard, J.-P. Locquet, E. Mächler, P. Martinoli and Ø. Fischer.
   The role of epitaxial strain in the properties of high T_c thin films.
   Proc. Microscopy and Microanalysis 1995, edited by G. W. Bailey, M. H. Ellisman, R. A. Hennigar and N. J. Zaluzec (Jones and Begell Publishing, New York, 1995), 382.

3. Y. Jaccard, T. Schneider, J.-P. Locquet, E. J. Williams, P. Martinoli and Ø. Fischer.
   Evidence for 3D-XY critical point behavior in $La_{2-x}Sr_xCuO_4$ films.
   Europhys. Lett. **34** (4), 281 (1996).

4. J.-P. Locquet, Y. Jaccard, A. Cretton, E. J. Williams, F. Arrouy, E. Mächler, T. Schneider, Ø. Fischer and P. Martinoli.
   Variation of the in-plane penetration depth λ_{ab} as a function of doping in $La_{2-x}Sr_xCuO_{4+\delta}$ thin films on $SrTiO_3$.
   Phys. Rev. B. **54**, 7481 (1996).

PROCEEDINGS REPRINT

SPIE–The International Society for Optical Engineering

Reprinted from

Oxide Superconductor Physics and Nano-Engineering

26–28 January 1994
Los Angeles, California

Volume 2158

Characterization of MBE-grown ultrathin films in the $La_{2-x}Sr_xCuO_{4\pm\delta}$ system

Y. Jaccard[a,b], A. Cretton[a,c], E.J. Williams[a,c], J.-P. Locquet[a],
E. Mächler[a], C. Gerber[a], T. Schneider[a], Ø. Fischer[c] and P. Martinoli[b]
[a]IBM Research Division, Zurich Research Laboratory, 8803 Rüschlikon, Switzerland
[b]Institut de Physique, Université de Neuchâtel, 2000 Neuchâtel, Switzerland
[c]Département de Physique de la Matière Condensée, Université de Genève, 1211 Genève, Switzerland

ABSTRACT

Using a molecular beam epitaxy deposition technique, c-axis $La_{2-x}Sr_xCuO_{4\pm\delta}$ ultrathin films have been prepared on (001) $SrTiO_3$ substrates. Several superconductive properties such as the critical temperature T_c, the penetration depth $\lambda_{ab}(0)$, the activation energy for flux flow ΔU and the Hall coefficient R_H are reported for the same set of films. As the dopant content is increased, maximum values for T_c and ΔU are observed near the optimum doping while R_H decreases continuously.

1 Introduction

High T_c superconductivity was originally discovered in the '214' system ($La_2CuO_{4\pm\delta}$) upon doping with Ba or Sr,[1] and this still remains an actively studied system. One major reason for the continued interest is that homogeneous samples can be prepared easily in either an underdoped and an overdoped state.[2] An additional degree of freedom may be provided by the insertion of extra oxygen into the undoped '214' lattice by changing the La/Cu ratio,[3] or a treatment at high pressure,[4] or by using electrochemical oxidation techniques.[5,6] Furthermore the compound is at the center of an ongoing debate regarding whether or not bulk superconductivity is restricted to a narrow compositional range[7] around the optimum doping. However Kitazawa[2] has demonstrated that *under well controlled preparation conditions* a broad doping range supports bulk superconductivity.

The penetration depth $\lambda_{ab}(0)$ is a parameter of fundamental interest which can provide insight into the superconductive pairing mechanism. This parameter has hitherto been derived from either μSR (muon-spin relaxation) measurements[8] or from 'mixed-state' magnetization isotherms[9] (i.e. in the high temperature reversible regime). Obtaining accurate values for $\lambda_{ab}(0)$ using the former method requires a careful analysis of the relaxation rate (beyond the simple Gaussian approximation) as well as the use of assumptions concerning the nuclear dipole fields, random displacements of the vortices out of their rigid-lattice positions and a distribution of demagnetization factors.[10] The latter method uses data from the small reversible $M(H)$ regime, close to T_c (for instance 26 to 28K[9]), to extrapolate the $\lambda_{ab}(T)$ to zero temperature using a two-fluid[2] or a BCS[9] temperature dependence. Very close to T_c a large diamagnetic effect induced by thermodynamic fluctuations influences the total magnetization M and a model derived by Hao and Clem[11] must be used to derive accurate values. Furthermore in the case of strong pinning (as in overdoped powder samples[2]) the temperature range where $M(H)$ is reversible becomes too small preventing a correct determination. Finally, data obtained from bulk samples yield an 'effective' penetration depth λ_{eff} which may be related to λ_{ab} when the anisotropy and the particle distribution are known.

0-8194-1453-0/94/$6.00

In this work we illustrate how $\lambda_{ab}(0)$ and the activation energy ΔU can be derived from mutual inductance data obtained in the temperature regime of 4.2K to T_c.

2 Experimental

The thin films were grown in an MBE system equipped with four effusion cells (one for strontium), two electron beam guns (copper and lanthanum), two quartz monitors, a quadrupole mass-spectrometer,[12] an RF plasma source[13] and a RHEED system. The base pressure of the (unbaked) system is $\simeq 10^{-9}$ Torr, while during the growth an orginal oxygen pressure of 1×10^{-5} Torr is used and subsequently reduced to approximately 2×10^{-6} Torr as a function of the La deposition rate. A sequential deposition process is used whereby the molecular beam flux ($\simeq$ 3-5 monolayers per minute for each source) is controlled by the mass-spectrometer which was previously calibrated using quartz monitors. The sensitivity of both monitoring techniques is of the order of 0.1% of a monolayer, however the drift of the mass-spectrometer during the growth limits the effective composition control to 1-5 %. This sensitivity is sufficient for the La and Cu layers, but since the Sr layer corresponds to a thickness between 0.07 and 0.30 monolayers, the effective accuracy of the Sr content is no better than 10-20%. For all the samples reported here the deposition conditions were similar i.e. a $SrTiO_3$ (001) substrate, a growth temperature of 750°C, an evaporation rate of 3-6 monolayers per minute, a sequential deposition starting with $2\text{-}x$ monolayers La, x monolayers Sr and 1 monolayer Cu followed by a 10 second waiting step under a continuous flow of atomic oxygen for each unit cell. During the 'cool-down' step the heater power is turned off completely and cooling takes place over more than two hours under the same flow of atomic oxygen until the pyrometer reads a temperature below 100°C. The final film thicknesses were all $\leq$ 50nm.

3 Results

During growth well defined RHEED patterns (see Fig. 1a) corresponding to epitaxial growth were observed. The in-plane lattice parameter was 0.38nm and the RHEED streaks revealed a nearly 2D surface structure. Crystal growth can proceed from either a La-rich or a Cu-rich compositon and for each case distinct features are observed. As in the case of $DyBa_2Cu_3O_7$, Cu_2O crystallites with the (110) plane parallel to the substrate surface can nucleate very easily on top of c-axis La_2CuO_4 under Cu-rich conditions. These are the origin of large scale precipitates and similarly shaped grains as those reported in[14] are observed. Their observation by RHEED is more difficult in the case of Sr-doped La_2CuO_4 as they react readily with subsequently deposited Sr and form a shell of small and polycrystalline impurities around themselves.

The surface morphology, observed using AFM, is in agreement with the RHEED observations. A predominantly 2D surface, with large atomically flat terraces (up to 0.3μm) and atomic steps (0.66 nm, i.e. one half unit cell) is observed, this is occasionally disturbed by the Cu-O precipitates (Fig. 1b). This $0.8\mu m \times 0.8\mu m$ AFM[15] image from a 50nm thick film clearly reveals that the growth for this compound under the discussed deposition conditions is very different from the spiral growth mechanism suggested by some authors[16] for the $DyBa_2Cu_3O_7$ compound.

X-ray diffraction experiments confirm a c-axis epitaxial growth and for all films reported here, finite size effect oscillations were observed around the *(00l)* peaks, allowing a good estimate of the total crystalline film thickness (Fig. 2). Such oscillations are not present in films containing large thickness fluctuations or a high density of impurities and growth spirals. The structural quality was further measured using Φ scans for the {103} planes. No peaks other than those derived from the four-fold symmetry of a pure c-axis thin film were found.

The microstructure was observed using TEM imaging of cross-section and plan view specimens[17] of an undoped '214' film. There is a misfit of $\simeq$ 3.5% between the film and substrate such that the film would be under tension. However as can be seen in Fig. 3a, which shows a bright field image from a plan view specimen of a '214' film, taken a few degrees away from the [001] zone such that the two component misfit dislocation network is imaged, a dislocation separation of $\simeq 14\pm2$nm can measured. This value is in good agreement with the 14.5 nm separation expected if the

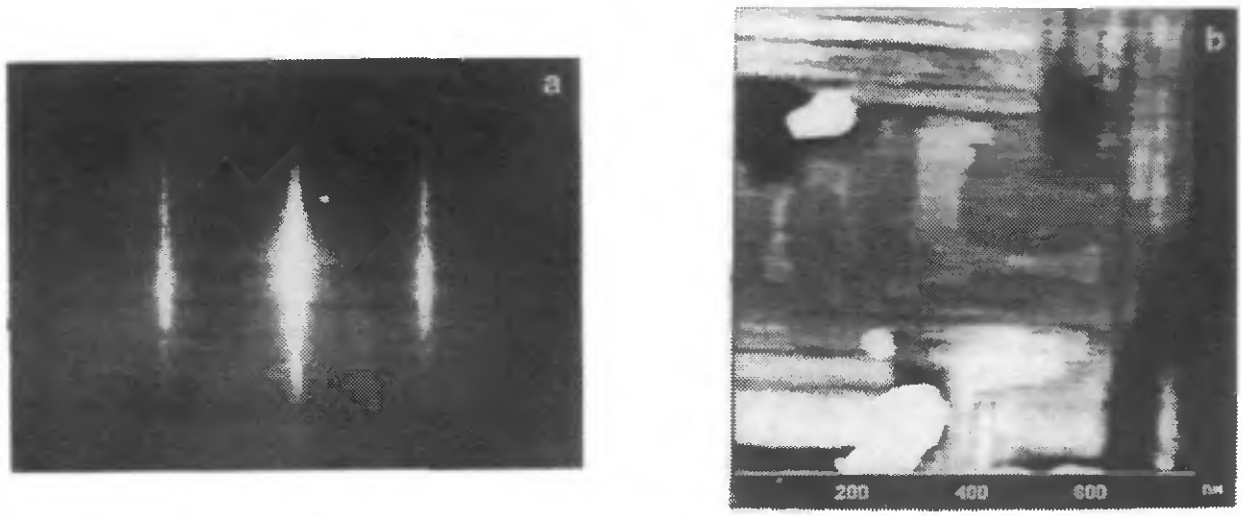

Figure 1: a) RHEED image of a growing 214 film; b) AFM picture showing atomically flat regions with 0.66 nm steps and Cu-O precipitates.

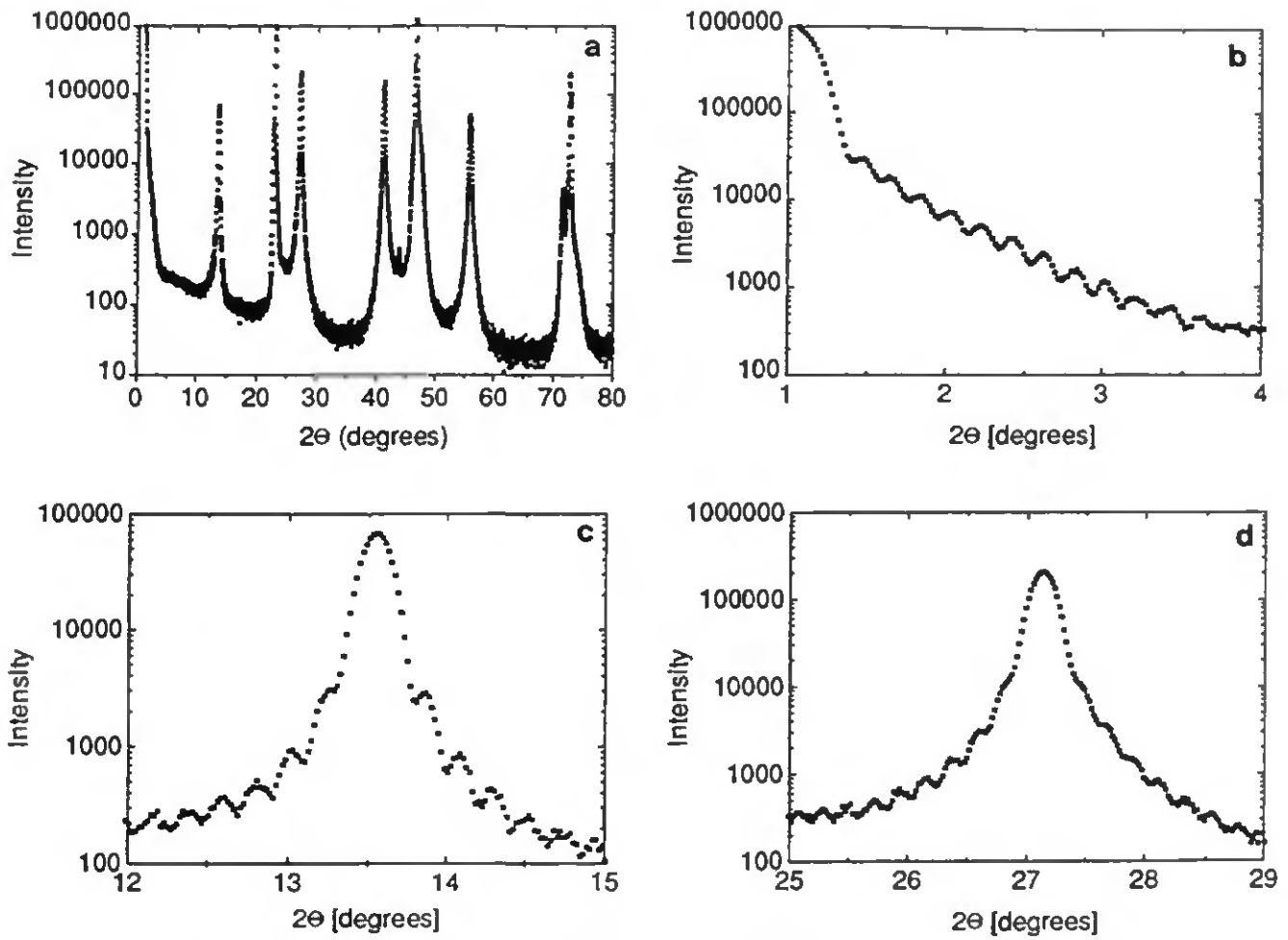

Figure 2: X-ray diffraction pattern showing a) a complete spectrum with only substrate and (00l) peaks; b) finite size effect oscillations at low angle; c) around the (002) reflection and d) around the (004) reflection.

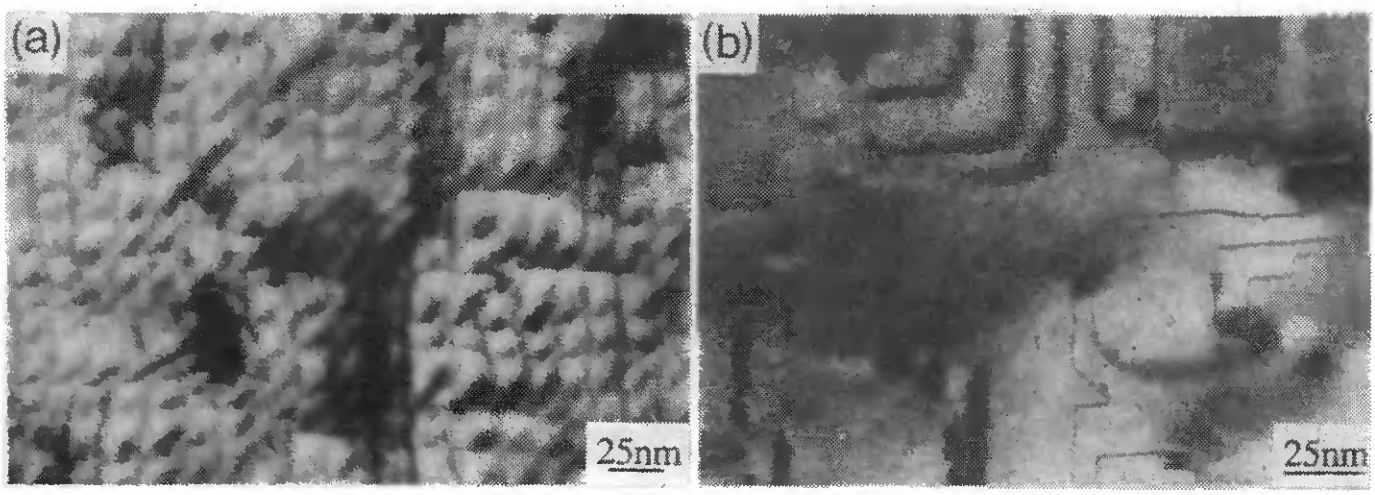

Figure 3: a) Bright field image taken a few degrees away from the [001] zone; b) 101_{LSCO} dark field image of a film taken near the [$\bar{1}$11] zone.

misfit were wholly accomodated by edge-type misfit dislocations with b=a/2<110> (a = a axis parameter) in the orthorhombic material.

Additionally planar faults have been observed to grow within both undoped and doped '214' films. These faults lie on the four {101} tetragonal or equivalent {111} orthorhombic planes and form a network across the whole film with a characteristic separation of 50±10nm (Fig. 3b). Cross-sectional specimens reveal that the faults penetrate the full thickness of the film starting at the substrate-film interface. Lattice imaging indicates that these faults contain a shear component which has as yet not been possible to quantify. There is some evidence that the faults originate at defects on the substrate surface, further their presence and position do no seem to be related to the Sr content or to the tetragonal to orthorhombic phase change. Clearly they are not twin boundaries which lie on {101} orthorhombic planes.[18]

The thickness of the grown '214' thin films was restricted to about 50nm, to allow an accurate measurement of λ using the two-coil mutual inductance measurements.[19] The critical temperature of thin '214' films is strongly dependent on the film thickness, for instance Kwo et al.[20] reported that films with T_c above 30K are obtained on $SrTiO_3$ (001) substrates only for thicknesses above 500nm in agreement with our own observations. Several authors have reported similar observations[21,22,23,24,25,26] each with a different maximum of the critical temperature. A related experimental trend has been shown in '214' superlattices,[27,28,29] but the real thickness dependence can be easily masked by the large total sample thickness.

The $T_c's$ of ultrathin films with and without a buffer layer are reported in Fig. 4a (T_c was taken as the temperature at which half the value of the resistivity above the onset was attained). These data were obtained from films which had been grown in two steps such that, on one half of the substrate a buffer-layer of 15 unit cells of undoped, hence insulating, '214' was grown (this thickness should be large enough to relieve all the strain and to nucleate the network of misfit dislocations), while the other half was covered with a shield. After deposition of the buffer-layer, the shield was removed (in-situ) and a '214' film with $x \simeq 0.15$ was deposited on the whole. The data in Fig. 4a show that ultrathin films on this substrate are not superconducting until a critical thickness of 10 unit cells is reached. Furthermore the films without a buffer-layer show that the T_c saturates for film thicknesses larger than $\simeq$ 20 unit cells, while those with a buffer-layer saturate at doped film thicknesses around 10 unit cells. Nevertheless these data correspond to the thinnest superconducting '214' films reported to date.

The dependence of the critical temperature on the strontium concentration is rather different for these films than for bulk material. As discussed above the large error in the strontium concentration during growth makes using that nominal value to compare samples with different content, unrealistic. In addition, even when the strontium

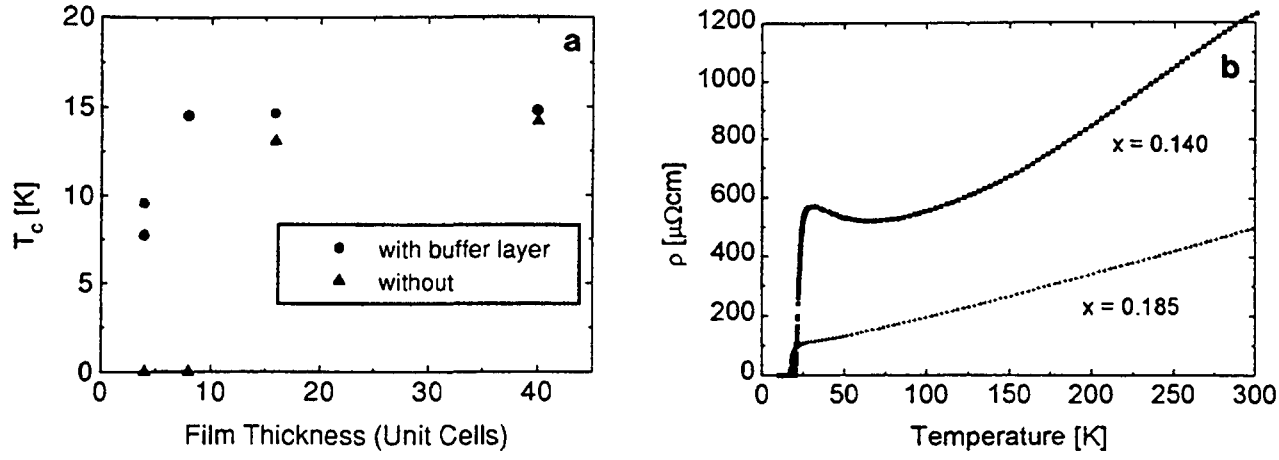

Figure 4: a) T_c versus the thickness of '214' films (x≃0.15) with and without an insulating buffer layer; b) $\rho_{ab}(T)$ for an underdoped and an overdoped film.

concentration is kept more constant during the deposition, as in the sputtering experiment of Suzuki,[25] approximately 300nm thick films with the same nominal strontium content are reported with T_c between 31.6K and 25.2K and ρ_{300K} values between 9 and 19×10^{-4} Ωcm. Since using the nominal values would not reflect the real strontium content another means of determination must be found. Here we have used the values of the resisitivity at 300 K, $\rho_{300K}(x)$ and the resistance ratios $\rho_{300K}/\rho_{60K}(x)$ and $\rho_{60K}/\rho_{30K}(x)$ which are all well defined functions of the strontium content x.[30,24,25,31] The $\rho(T)$ values of our films lie close to the thin film data of Suzuki[24,25] allowing a comparison of the three parameters $\rho_{300K}(x)$, $\rho_{300K}/\rho_{60K}(x)$ and $\rho_{60K}/\rho_{30K}(x)$. In Fig. 4b the $\rho_{ab}(T)$ data for an underdoped and an overdoped film are shown. Since these strontium content dependences are well defined, a relation $x_c = f(\rho_{300K}, \rho_{300K}/\rho_{60K}, \rho_{60K}/\rho_{30K})$ can be constructed where x_c is a calculated effective strontium content estimated from the transport properties of our thin films. The x_c values derived using this method are those used throughout this paper.

The dependence of critical temperature (T_{c0}) values on x_c is shown in Fig. 5 for three series of samples prepared under identical conditions but with a total thickness of 30, 39 and 50nm respectively (all greater than the critical thickness mentioned above). The maximum observed critical temperature is about 22K for x_c approximately 0.17 and as for bulk materials, away from optimum doping, the critical temperature decreases. It is not yet clear which physical mechanism limits the critical temperature to values below 30K in thin films of this system. There are at least four different structural phases in the '214' system, these all support superconductivity albeit with a different T_c as the structural details, such as the octahedral tilting angle and the orthorhombicity, are changed.[32] Both these parameters are not known for the reported thin films since x-ray diffraction and TEM could not resolve the a and b lattice parameters. The presence of misfit dislocations indicates that the film 'feels' the substrate very strongly and it might thus be assumed that the structural phase transformations from the tetragonal structure of the film at high temperature into any of the lower symmetry phases (orthorhombic for instance) are influenced by the cubic substrate. In the light of this it could be suggested that the highest T_c in the '214' compound with tetragonal structure is $\simeq$ 28K and that only much thicker films (800nm),[20] allowing a more optimal phase transformation, have a higher T_c.

A good check for the accuracy of the estimated Sr content (x_c) is provided by comparing the Hall coefficient, R_H, of the films with values in the literature. In Fig. 6a the R_H is plotted against temperature for films of thickness 50 nm, while Fig. 6b relates R_H to x_c at a fixed temperature (72K). Within the scatter of the data, increasing x_c monotonically decreases R_H (and thus increases the effective carrier density). Uchida[33] points out that *the '214' compound is a system in which the carrier density n_N is definitely equal to the Sr content.* The carrier density estimated using the simple one carrier one band relation ($R_H = e \times n_N$) gives for $x_c \simeq 0.12$, $n_N \simeq 10^{21}/\text{cm}^3$ and for $x_c \simeq 0.2$, $n_N \simeq 8 \times 10^{21}/\text{cm}^3$, i.e. an eightfold increase in carrier density for a doubling in x_c. This contrast confirms that the simple band relation does not provide a correct estimate of n_N, as was previously reported.[24] However more

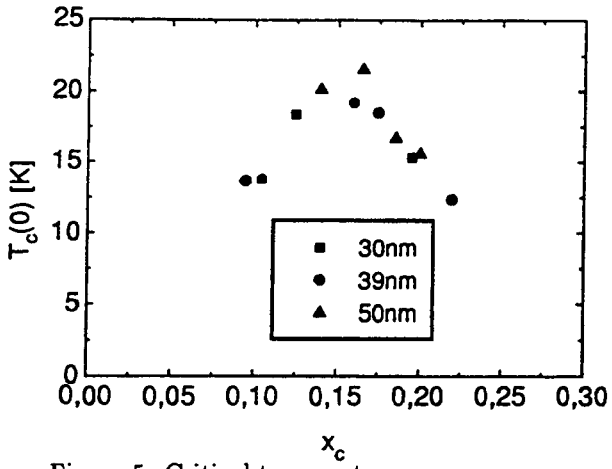

Figure 5: Critical temperature versus x_c.

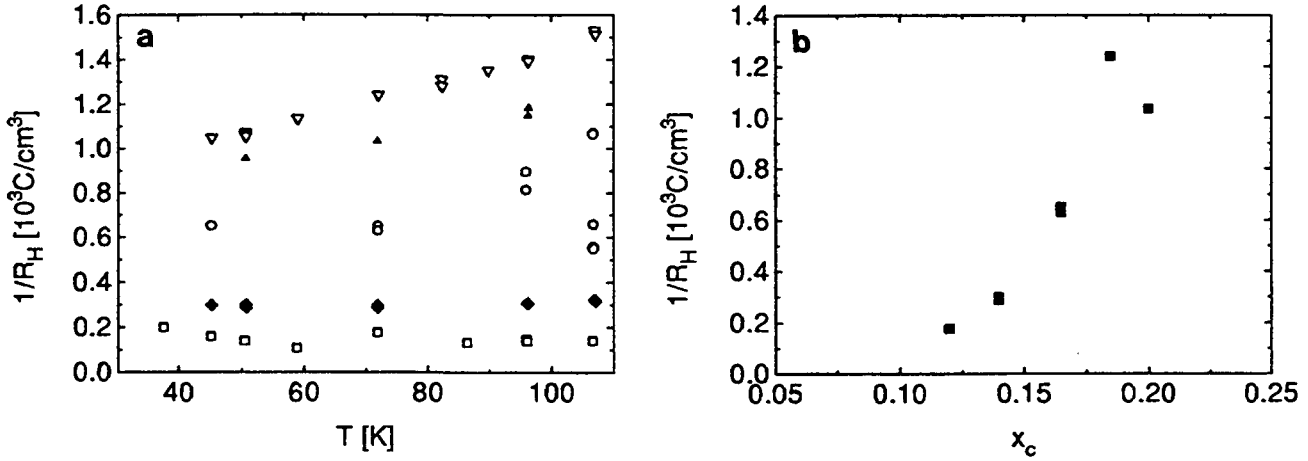

Figure 6: a) Hall coefficient R_H^{-1} against the temperature for the 50 nm thick films with $x_c = 0.12(\square)$, $0.14(\blacklozenge)$, $0.165(\circ)$, $0.185(\triangledown)$, $0.2(\blacktriangle)$; b) Hall coefficient R_H^{-1} at 72K versus x_c

complex theoretical treatments like the one which relates R_H to the energy dispersion of the upper Hubbard band of the Cu d_{z^2} band as a function of Sr content, might accurately explain the experimental data.[34] The Hall coefficient for our film closest to optimum doping $x_c \simeq 0.16$, is nearly identical to the those found in other reports,[24,35] thus confirming the use of x_c as an estimate of the true Sr content. However, most importantly, this value proves that the origin of the reduced T_c in our films is not related to a problem with the doping and the normal state carrier density.

A plot of the real and imaginary parts of the mutual inductance signal (taken at a frequency of 1kHz) against temperature can be seen in Fig. 7a for a field of 0 and 0.4 T respectively. At low temperature the imaginary part, containing the superfluid background (and in an applied field contributions from vortex pinning), becomes constant indicating that the screening currents and the field penetration saturate. The real part measures all dissipative processes (vortex motion and eddy currents) and is close to zero except for the transition region close to T_c. From these two signals using a numerical inversion procedure,[19] an inductance L_K and a sheet resistance $R_\square$ can be deduced. The penetration depth $\lambda_{ab}(T)$ (in Å) is related to L_K (in nΩ) using $L_K = \mu_0 \lambda_{ab}^2/d$ with μ_0 the vacuum permittivity ($1.257\ 10^{-7}$nH/Å) and d the film thickness (in Å), while the resistivity $\rho_{ab}(T)$ (in nΩcm) is related to $R_\square$ (in nΩ) using $\rho_{ab} = R_\square \times d \times 10^{-8}$.

Curves of the resistivity $\rho_{ab}(T)$ and the inductance $L_K(T)$ obtained using the numerical inversion from the two-coil mutual inductance measurement of the previously mentioned film, are shown in Fig. 7b and Fig. 7d, respectively for

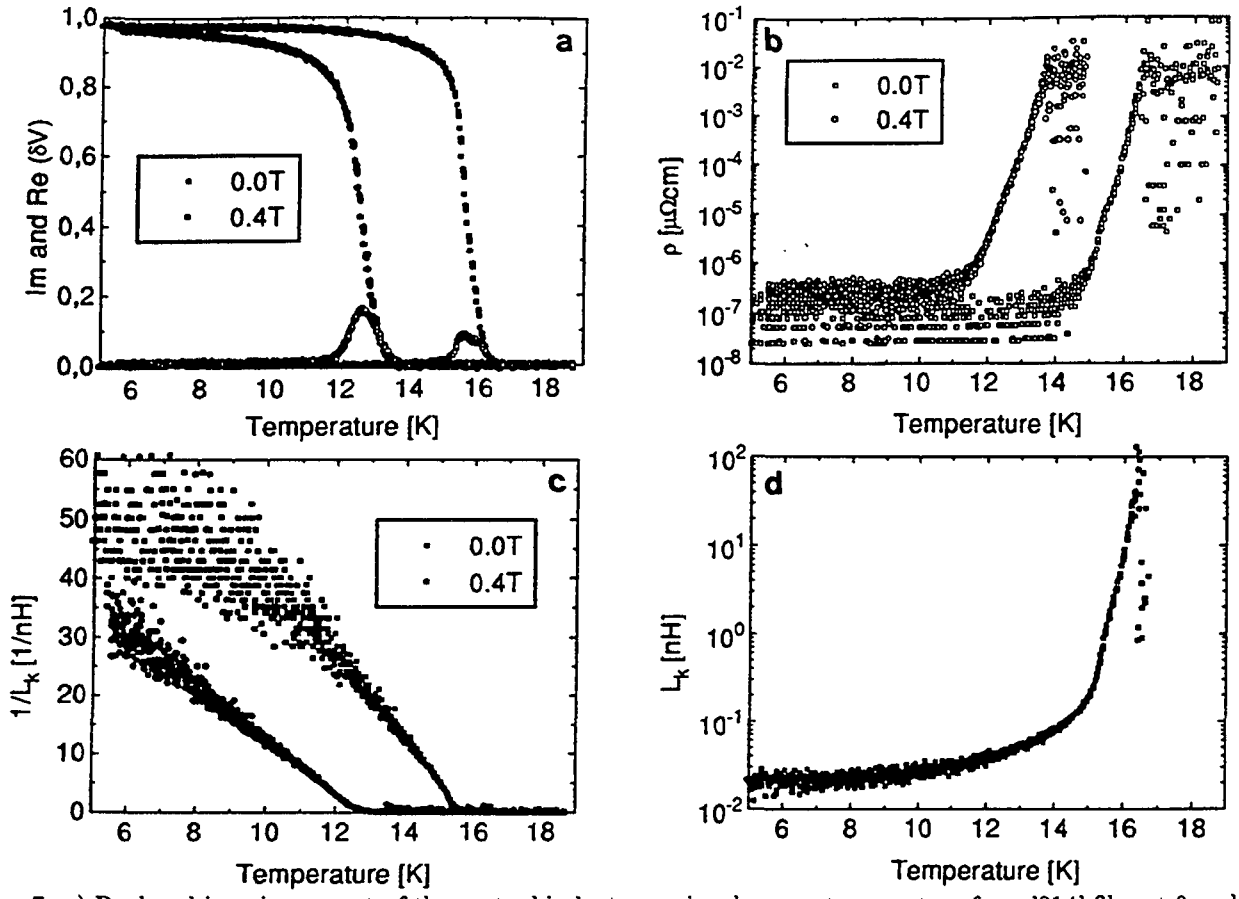

Figure 7: a) Real and imaginary part of the mutual inductance signal versus temperature for a '214' film at 0 and 0.4 Tesla; Temperature dependence of b) the resistivity ρ_{ab}, c) the inverse inductance and d) the 'zero' field inductance (proportional to λ^2).

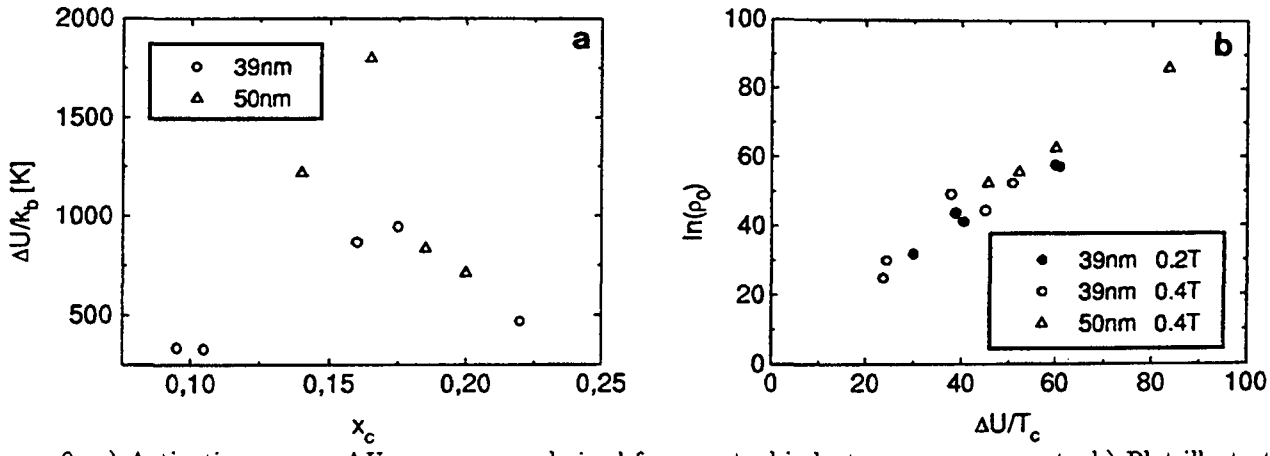

Figure 8: a) Activation energy ΔU versus x_c as derived from mutual inductance measurements; b) Plot illustrating the 'linear' relation between $\ln(\rho^0_{ab})$ and $\Delta U/T_c$ with ΔU here in Kelvin.

0 and 0.4T. The large shift of $\rho_{ab}(T)$ and $\lambda_{ab}(T)$ (3K) caused by the change in the magnetic field parallel to the c-axis is either due to a weak critical field H_{c2} or to a weak pinning and thermally activated flux flow (TAFF) of individual vortices. In particular, the broadening of the resistive transition as the field is increased is evidence for the latter suggestion. Suzuki et al.[25] reported the magnetoresistance of '214' films up to 12 T, they show that for underdoped samples an increase in the field produces a strong broadening of the $\rho_{ab}(T)$ curves, while for the overdoped samples little broadening occurs but rather a parallel shift of the curves. Clearly the magnetic field used for our preliminary study is not strong enough to confirm their observation. Therefore we restrict our analysis to the TAFF model which writes the resistivity $\rho_{ab}(T,H) = \rho^0_{ab} \exp(-\Delta U(T,H)/k_B T_c)$ i.e. as a thermally activated function with an activation energy ΔU dependent on temperature and field. It has been pointed out by Kes[36] that the *activation energy should decrease as the anisotropy of the material increases.* In the TAFF language, the anisotropy is proportional to the inverse 'flux' correlation length L_c via the qualitative relation $\Delta U = p(\mu_0 H_c^2/2) R_c^2 L_c$ where p is a fraction of the condensate energy density and R_c is the 'flux' correlation length perpendicular to the magnetic field. Since the anisotropy (reflected for instance in the ratio ρ_c/ρ_{ab}) in the Sr doped '214' system changes drastically as the doping increases (ρ_c/ρ_{ab} is about 4000 for $x \simeq 0.06$ and about 160 for $x \simeq 0.3$)[37,38] this system is ideal to test the prediction of Kes.[36] Another manner to artificially change the anisotropy was achieved in a study of $YBa_2Cu_3O_7$/ Pr $Ba_2Cu_3O_7$ superlattices[39] and the above conjecture was verified for that system. Furthermore a general relationship between ρ^0_{ab} and ΔU, valid for various fields and samples, was suggested.

The activation energies derived from mutual inductance measurements are presented in Fig. 8a as a function of x_c. In this figure the activation energy reaches a maximum for optimum doping and becomes small away from the optimum. As far as the underdoped regime is concerned, as doping increases (and anisotropy decreases) the model of Kes[36] predicts an increase of the activation energy and this is corrobated by the experimental data. In the overdoped regime, however, the change in anisotropy is not very large as the Sr content increases but since the superconductor behaves more like a 'normal' superconductor its critical field H_{c2} (and therefore H_c) is strongly reduced (as reported for instance by Suzuki et al.[25]). We suggest that this mechanism is responsible for the decrease of the activation energy at high doping.

Feigel'man et al.[40] propose in a quantitative model that the activation energy of a dislocation pair in the collective pinning model behaves such that $\Delta U = (\Phi_0^2 d/16\pi^2\mu_0\lambda^2)\ln(a_0/\xi)$, where a_0 is the flux-line lattice spacing and ξ the correlation length. Since $a_0/\xi \gg 1$, the logarithmic term is only a slowly varying function of the Sr concentration. Therefore the behavior of the activation energy versus Sr content should be essentially that of $1/\lambda^2$ and this predicts a parabolic dependence for the latter. In Fig. 8b, $\ln(\rho^0_{ab})$ is plotted against $\Delta U/T_c$ and, as in the case of the $YBa_2Cu_3O_7$/ Pr $Ba_2Cu_3O_7$ superlattices, a straight line with a slope close to 1 is observed. This proves that the same 'vortex' physics (illustrated here using the TAFF model) is applicable to different cuprate superconductors and to high (90K) as well as relatively low (20K) transition temperatures.

Fig. 7d. shows the temperature dependence of the inductance $L_K \propto \lambda^2_{ab}$ measured using the mutual inductance technique. Except for the temperature regime close to T_c (where critical fluctuations play an important role), the temperature dependence can be fitted reasonably well with $\lambda(T)/\lambda(0) = [1-(T/T_c)^\nu]^{-1/2}$, where the exponent ν is either 1, 3/2 (for the ideal Bose gas or as an approximately BCS formula[41]) and 2 (empirical formula).[9] In the '214' system all these exponents, as well as the two-fluid exponent (4), have been observed so far and the origin of the variation is ambiguous. For instance, for the single crystal study of Li,[9] an exponent of 2 or 3/2 was suggested; while in the thin film study of Chang[42] an exponent close to 1 was found and measurements on bulk powders were interpreted using the two-fluid model.[2] The temperature dependence remains a subject of strong debate as it should reveal the symmetry of the superconducting gap function Δ_k. A calculation using a simple model taking a 'small' distribution of T_c and $\lambda_{ab}(0)$ (each about 20%) around the average values, but with a fixed temperature dependence $\nu = 4$, produced a curve with an effective exponent close to 2. However, and most importantly, the derived $\lambda_{ab}(0)$ remains very close to the average value. Here we do not suggest a particular exponent ν, nor that a temperature dependence different from the two-fluid model is necessarily a proof for inhomogeneity, but rather that the low temperature value $\lambda_{ab}(0)$ is rather insensitive to this inhomogeneity. Effectively at low temperatures the $\lambda_{ab}(T)$ of the different spatial regions are all saturating (except for the unlikely case where a distribution of T_c down to 0K and $\lambda_{ab}(0)$ up to ∞ is assumed).

It is important to point out that most values for $\lambda_{ab}(0)$ found in the literature are obtained using $M(H)$ values in the small temperature regime where reversibility still applies. In that case the determination of the correct exponent

is rather difficult and so hence is the determination of $\lambda_{ab}(0)$. In Fig 7d. the $\lambda_{ab}(0)$ value derived from the mutual inductance technique, using an exponent $\nu = 3/2$,is (7250 $\pm$ 700) Å. The error bar originates partially from the scatter in the data (see the low temperature regime of Fig 7d.) and were chosen to be large enough to include fits using exponent values between $\nu = 1$ and 2. A detailled analysis of the penetration depth versus doping will be reported in a subsequent paper.[43]

Finally in the table below we have listed the major experimental parameters related to the thin films discussed in this paper.

Samples	x_c	T_c[K]	ΔU[K](0.4T)	Δ U[K](0.2T)	$R^{-1}_{H_{72K}}[10^3 C/cm^3]$
LC37	0.195	12.65	-	-	-
LC85	0.125	18.53	-	-	-
LC59	0.22	10.6	465	477	-
LC62	0.095	11.8	334	410	-
LC63	0.105	13.15	327	557	-
LC68	0.16	19.36	866	1170	-
LC69	0.175	18.17	942	1110	-
LC96	0.12	16.39	-	-	0.175
LC97	0.165	21.59	1798	-	0.639
LC98	0.2	14.1	709	-	1.032
LC104	0.14	20.3	1218	-	0.293
LC106	0.185	16.05	834	-	1.238

4 Acknowledgements

The authors wish to thank K.A. Müller, J.G. Bednorz, J.-M. Triscone, D. Ariosa and R. Micnas for stimulating discussions and the Swiss National Science Foundation for financial support through the PNR30 program.

5 REFERENCES

[1] J.G. Bednorz and K. A. Müller, Z. Phys. **B64**, 189 (1986).

[2] K. Kitazawa, T. Nagano, Y. Nakayama, Y. Tomioka and K. Kishio, "Applied Superconductivity" **1** (1993) 567. T. Nagano, Y. Tomioka, Y. Nakayama, K. Kishio and K. Kitazawa, Phys. Rev. **B48**, 9689 (1993).

[3] P.M Grant, S.S.P. Parkin, V.Y. Lee, E.M. Engler, M.L. Ramirez, J.E. Vazquez, G. Lim, R. D. Jacowitz and R.L. Greene, Phys. Rev. Lett.**58**, 2482 (1987) ; S. M. Fine, M. Greenblatt, S. Simizu and S. A. Friedberg, "Chemistry of high-temperature superconductors, chapter 10, 95 (1987)

[4] J. Beille, R. Cabanel, C. Chaillout, B. Chevalier, G. Demazeau, F. Deslandes, J. Etourneau, P. Lejay, C. Michel, J. Provost, B. Raveau, A. Sulpice, J.-L. Tholence and R. Tournier, Compt. Rend. Acad. Sci. (Paris), **304** (1987) 1097; P. M. Grant, S. S. P. Parkin, V. Y. Lee, E. M. Engler, M. L. Ramirez, J. E. Vazques, G. Lim, R. D. Jacowitz and R. L. Green, Phys. Rev. Lett. **58** (1987) 2482.

[5] A. Wattiaux, J.-C. Park, J.-C. Grenier and M. Pouchard, Compt. Rend. Acad. Sci. (Paris) **310** (1990) 1047 ; J.-C. Grenier, A. Wattiaux, N. Lagueyte, J.-C. Park, E. Marquestaut, J. Etourneau and M. Pouchard, Physica **C 173** (1991) 139.

[6] J.-P. Locquet, E. Mächler, E.J. Williams, A. Cretton, Y. Jaccard and C. Gerber, Applied Physics **A57**, 211 (1993).

[7] R.B. Van Dover, R.J. Cava, B. Batlogg and E.A. Rietman, Phys. Rev. **B35** (1987) 5337 ; K. Yoshimura, Y. Nishizawa, Y. Ueda and K. Kosuge, J. Phys. Soc. Jpn. **59** (1990) 3073.

[8] Y.J. Uemura et al., Phys. Rev. Lett. **62**, 2317 (1989) and Phys. Rev. **B38**, 909 (1988).

[9] Q. Li, M. Suenaga, T. Kimura and K. Kishio, Phys. Rev. B**47**, 2854 (1993).

[10] P. Birrer, F.N. Gygax, B. Hitti, E. Lippelt, A. Schenck, M. Weber, D. Cattani, J. Cors, M. Decroux and Ø. Fischer, Phys. Rev. **B48**, (1993) 16589.

[11] Z. Hao, J.R. Clem, M.W. McElfiesh, L. Civale, A.P. Malozemoff and F. Holtzbeg, Phys. Rev.**B46**, 2844 (1991); Z. Hao and J.R. Clem, Phys. Rev. Lett. **67** 2371 (1991).

[12] The mass-spectrometer is an instrument from Hiden Analytical, Warrington, England.

[13] J.-P. Locquet and E. Mächler, J. Vac. Science & Technology, A3100 (1992). The atomic oxygen source is an instrument from Oxford Applied Research, Crawley Mill, Oxfordshire, England.

[14] J.-P. Locquet, Y. Jaccard, C. Gerber and E. Mächler, Appl. Phys. Lett. **63**, 1426, (1993).

[15] The AFM instrument is a Digital Instruments Nanoscope III, Santa Barbara CA, USA.

[16] C. Gerber, D. Anselmetti, J.G. Bednorz, J. Mannhart and D. Schlom, Nature, **350**, 279 (1991).

[17] E.J. Williams, J.-P. Locquet, E. Mächler, Y. Jaccard, A. Cretton, R.F. Broom, C. Gerber, T. Schneider, P. Martinoli and Ø. Fischer, Proc. Electron Microscopy and Analysis Group Conf. "EMAG '93", Liverpool, U.K. Sept 14-17, 1993, p 329

[18] C.H. Cheng, S.-W. Cheong, D.J. Werder, A.S. Cooper, L.W. Rupp Jr. Physica C**175**, 301 (1991).

[19] B. Jeanneret, J. L Gavillano, G. A. Racine, Ch. Leemann and P. Martinoli, Appl. Phys. Lett. **55**, 2336 (1989).

[20] H.L. Kao, J. Kwo, R.M. Fleming, M. Hong and J.P. Mannearts, Appl. Phys. Lett. **59**, 2748 (1991).

[21] M. Y. Chern, A. Gupta and B. W. Hussey, Appl. Phys. Lett. **60**, 3045 (1992).

[22] H. Sato, M. Naito, T. Arima and Y. Tokura, Appl. Phys. Lett. **61**, 2470 (1992).

[23] H. Sato et al., private communication.

[24] M. Suzuki, Phys. Rev. B**39**, 2312 (1989).

[25] M. Suzuki and M. Hikita, Phys. Rev. B**44**,249 (1991).

[26] G.-C. Yi, W. Jo, Y.K. Kim, T.W. Noh, D.-K. Ko, H. Noh and Z.G. Kim, Physica C**194**, 293 (1992).

[27] H. Tabata, T. Kawai and S. Kawai, Appl. Phys. Lett. **58**, 1443 (1991).

[28] K. Horiuchi, T. Kawai, S. Kawai, Y. Fujiwara and S. Hirotsu, Physica C**209**, 531 (1993).

[29] T. Tabata, T. Kawai and S. Kawai, Phys. Rev. Lett **70**, 2633 (1993).

[30] H. Takagi, B. Batlogg, H.L. Kao, J. Kwo, R.J. Cava, J.J. Krajewski and W.F. Peck,Jr., Phys. Rev.Lett. **69**, 2975 (1992).

[31] Y. Nakamura and S. Uchida, Phys. Rev. B**47**, 8369 (1993).

[32] Wu. Ting and K. Fossheim, Phys. Rev. B**48**, 16751 (1993).

[33] S. Uchida, Jpn. J. Appl. Phys, **32**, 3784 (1993).

[34] H. Ushio, T. Schimizu and H. Kamimura, J. Phys. Soc. Jpn. **60** 1445 (1991).

[35] H.Y. Hwang, B. Batlogg, H. Takagi, H.L. Kao, J. Kwo, R.J. Cava, J.J. Krajewski and W.F. Peck, Jr. preprint.

[36] P.H. Kes and J. van den Berg, in 'Studies of High Temperature Superconductors', edited by A. Narlikar (Nova Science Publishers, New York, 1990), Vol. 5, p83.

[37] T. Kimura, K. Kishio, T. Kobayashi, Y. Nakayama, N. Motohira, K . Kitazawa and K. Yamafuji, Physica C**192**, 247 (1992).

[38] Y. Nakamura and S. Uchida, Phys. Rev. B**47**, 8369 (1993).

[39] O. Brunner, L. Antognazza, J.-M. Triscone. L. Miéville and Ø. Fischer, Phys. Rev. Lett. **67**, 1354 (1991).

[40] M. V. Feigel'man, V.B. Geshkenbein and A.I. Larkin, PhysicaC**167**, 177 (1990).

[41] J.R. Clem, Ann. Phys. (N.Y.) **40**,268 (1966).

[42] A.M. Chang, H.D. Hallen, H.F. Hess, H.L. Kao, J. Kwo, A. Subdø and T.Y. Chang, Europhys. Lett. **20**, 645 (1992).

[43] J.-P. Locquet et al, to be published.

THE ROLE OF EPITAXIAL STRAIN IN THE PROPERTIES OF HIGH T_C THIN FILMS

E.J. Williams,*,** A. Cretton,*,** Y. Jaccard,*,*** J.-P. Locquet,* E. Mächler,* P. Martinoli,*** and Ø. Fischer**

*IBM Research Division, Zurich Research Laboratory, CH–8803 Rüschlikon, Switzerland
**D.P.M.C. Université de Genève, CH–1211 Genève, Switzerland
***Institut de Physique, Université de Neuchâtel, CH–2000 Neuchâtel, Switzerland

The difference observed between the critical temperatures measured for bulk material or very thick films (>500 nm for the '214' system) and those measured for thin films (<65 nm) has long been of curiosity. Thin films never attain the high values of T_c achieved in bulk or thick film material. Various mechanisms have been proposed to explain this phenomenon, for example Kosterlitz–Thouless effects, inadequate or unstable oxygenation, and strain itself. Formally the role of strain has remained insubstantiated.

The system on which we have concentrated our efforts is that of $La_{2-x}Sr_xCuO_4$ (LSCO) deposited using MBE, mainly onto (001) $SrTiO_3$ (STO) substrates. These films have been grown at about 700°C at $\sim 3 \times 10^{-6}$ torr oxygen pressure and cooled after growth at $\sim 10°\,min^{-1}$. The films have subsequently been examined using several microstructural and electronic probes, including x-ray diffraction, AFM, resistivity, Hall effect and kinetic inductance.[1] The initial observations made by transmission electron microscopy revealed the films to have a unique orientation relation with the substrate such that for the orthorhombic nomenclature (ortho.) (001)LCO||(001)STO & (110)LCO||(100)STO. A number of other microstructural features were revealed including a network of interfacial misfit dislocations which were found to be edge type and to have $\mathbf{b}=a/2\langle 110\rangle_{ortho.}$.[2] These first observations of misfit dislocations with an $\sim 14 \pm 2$ nm spacing in a specimen with $x=0$ and 30 nm film thickness led us to believe that the films were probably well relaxed since from the room temperature powder diffraction data of undoped film material and substrate, an expected dislocation spacing of 14.5 nm can be calculated. At this stage the only possible influence envisaged of the dislocations on the electronic properties of the thin film was that resultant from the strain fields surrounding the dislocation cores. As can be seen from the 220ortho. dark field of a cross-sectional specimen of an undoped film shown in Fig. 1 and the disturbance of the contrast of the lattice image of the undoped film shown in Fig. 2, the strain fields penetrate some 2–6 unit cells into the film. However as our studies proceeded, films with varying Sr content $0<x<0.22$ were examined. As the Sr content of LSCO increases, the bulk a and b lattice parameters decrease, the crystal transforms from orthorhombic to tetragonal at $x \approx 0.05$, and the subsequent a parameter continues to decrease (meanwhile, c increases).[3,4] This reduction of the in-plane lattice parameters increases the intrinsic misfit between the LSCO and the STO and so might be expected to reduce the misfit dislocation spacing; for a fully relaxed film of $x=0.2$ the expected dislocation spacing is 11.1 nm. This reduced spacing has, however, not been observed as yet. From Fig. 3, a 220tet. dark field image from a plan view specimen of an $x=0.16$ film, and from Fig. 4, the 200tet. dark field of the same film, it can be seen that although the misfit dislocation array is not completely regular, the spacing is around 14 ± 1.5 nm.

A possible explanation for this large misfit dislocation spacing lies with the growth temperature. If the lattice parameters for the substrate and films expected at the growth temperature are compared, it is found that for both undoped and highly doped materials, misfit dislocation spacings of 14.3–14.7 nm are expected. This indicates that the interface structure formed during growth changes very little on cooling, and thus that cooled films are subject to a tensile strain within their plane proportional to the differential thermal expansivities of the materials. This also follows the trends expounded by Speck et al.[5] This in-plane tensile strain implies, via the Poissons ratio, that the c-axis of the films should be less than that observed in the bulk and exactly this has been observed in our x-ray data.[6] This all points to the necessity of considering the operation of the pressure effect in the reductions of T_c of these very thin film materials, even when their thicknesses are greater than the critical thickness.[7]

Proc. Microscopy and Microanalysis 1995, edited by G.W. Bailey, M.H. Ellisman, R.A. Hennigar, and N.J. Zaluzec

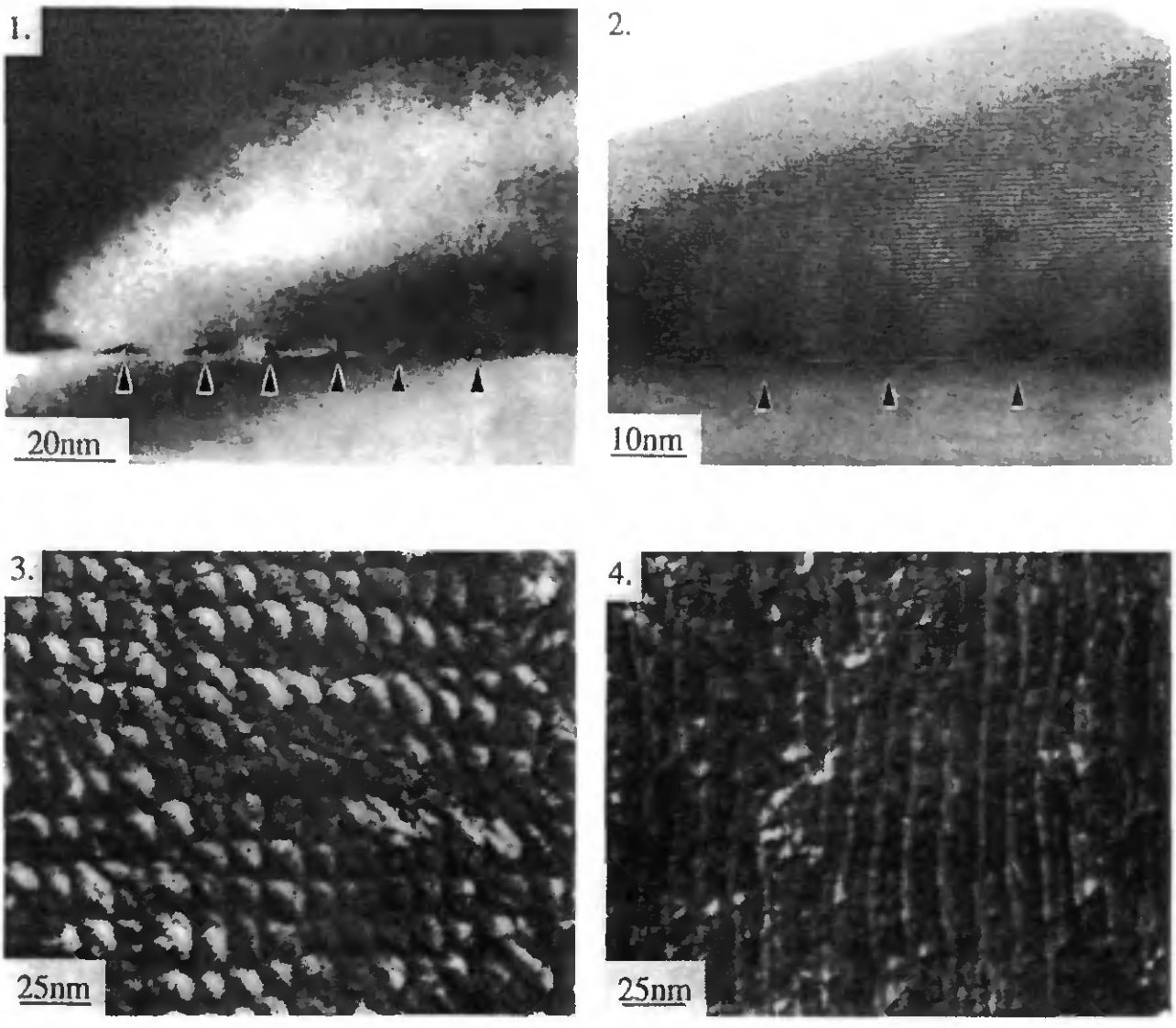

FIG. 1. 220LCO dark field image from a cross section showing strain contrast from misfit dislocations.
FIG. 2. Lattice image from undoped material showing disturbed contrast related to misfit dislocations.
FIG. 3. 220 dark field image from plan view of x=0.16 material showing the network of misfit dislocations.
FIG. 4. 200 dark field image from same specimen as in Fig. 3 showing that, although the dislocations are not entirely evenly spaced, their separations are ~14 nm.

References

1. Y. Jaccard et al., *SPIE Conf. on Oxide Supercond. Phys. & Nanoeng.* (1994).
2. E.J. Williams et al., *Inst. Phys. Conf. Ser.* 138:7(1993)329.
3. M. Braden *Ph.D. Thesis*, Köln (1992).
4. F. Tresse, *Ph. D. Thesis*, Bordeaux (1990).
5. J.S. Speck et al., *J. Appl. Phys.* 76(1994)447.
6. J.-P. Locquet et al., *Phys. Rev. B.* (submitted).
7. The authors would like to thank the Swiss National Science Foundation for financial support under the NFP30 Program.

EUROPHYSICS LETTERS 1 May 1996

Europhys. Lett., **34** (4), pp. 281-286 (1996)

Evidence of 3D-XY critical behaviour in $La_{2-x}Sr_xCuO_4$ films

Y. JACCARD[1,2], T. SCHNEIDER[1], J.-P. LOCQUET[1], E. J. WILLIAMS[1,3], P. MARTINOLI[2] and Ø. FISCHER[3]

[1] *IBM Research Division, Zurich Research Laboratory - 8803 Rüschlikon, Switzerland*
[2] *Institut de Physique, Université de Neuchâtel - 2000 Neuchâtel, Switzerland*
[3] *Département de Physique de la Matière Condensée, Université de Genève 1211 Genève, Switzerland*

(received 21 December 1995; accepted 12 March 1996)

PACS. 74.20−z – Superconductivity: theory.
PACS. 74.25−q – General properties; correlations between physical properties in normal and superconducting states.
PACS. 74.72Dn – La-based compounds.

Abstract. – We report measurements of the "zero field" ac sheet impedance $Z = R + i\omega L_k$ for thin, c-axis–oriented $La_{2-x}Sr_xCuO_4$ films. For sufficiently thin films of thickness d, the magnetic penetration depth λ_{ab} is given by $L_k = \lambda_{ab}^2/d$. We find that the temperature and intriguing doping dependence of L_k as well as the amplitude of the perpendicular real-space phase correlation length ξ_{c0}^{φ} are fully consistent with the critical behaviour of the three-dimensional XY model and finite-size scaling. Moreover, invoking finite-size scaling, we determine the value of the critical amplitude of ξ_{c0}^{φ}.

It has been recognized for some time that the small correlation length in high-temperature superconductors allows the observation of thermal fluctuation effects and hence of critical scaling behaviour near the superconducting phase transition [1]-[4]. Because for an extreme type-II superconductor the effective charge in the Ginzburg-Landau theory is negligibly small outside an inaccessibly small region close to the transition temperature T_c [3], [4], the order parameter is essentially neutral and in the simplest case corresponds to a complex scalar. This gives rise to fluctuations in the universality class of the three-dimensional (3D) XY model [5]. Indeed measurements of various properties, including specific heat [4], [6], [7] and magnetic penetration depth [8]-[10], strongly suggest that in the Meissner phase and close to the transition temperature, the fluctuations of the order parameter are essentially those of the 3D-XY model [8]. As of today, however, no systematic experimental study of the doping dependence of critical scaling properties, including finite-size scaling, and the relevance of disorder has been made.

In this letter we report kinetic-inductance measurements of the in-plane magnetic penetration depth $\lambda_{ab}(T)$ near T_c of $La_{2-x}Sr_xCuO_4$ films, which are sufficiently thin to reveal finite-size effects. The Sr doping allows us to cover the underdoped, optimally doped, and

overdoped regimes. We show that our measurements are fully consistent with 3D-XY critical behaviour and finite-size scaling in the entire doping range. Then we can extract the doping dependence of the perpendicular real-space phase correlation length ξ_{c0}^{φ}.

We used a two-coil mutual-inductance technique in zero field, which yields the ac sheet impedance $Z = R + i\omega L_k$. For thin films of thickness d, the magnetic penetration depth then follows from $L_k = \lambda_{ab}^2/d$ [11]. This technique is particularly well suited for accurate measurements close to the critical temperature. The film thicknesses have been chosen to cover part of the 3D critical fluctuation regime and the crossover to 2D behaviour. In this context, it is useful to define the various temperature regimes. Films are finite in one spatial direction, which in our case is perpendicular to the layers. For this reason, they will exhibit a Kosterlitz-Thouless (KT) phase transition at the temperature $T_{KT}(d)$, which depends on the film thickness d. In the bulk limit ($d \to \infty$) with transition temperature T_c, the system crosses over to the 3D-XY critical point. Indeed, the real-space phase correlation length perpendicular to the layers, $\xi_c^{\varphi}(T)$, cannot exceed the film thickness d, so that close to the 3D-XY critical point we have $\xi_c^{\varphi} = \xi_{c0}^{\varphi}|t|^{-\nu} \leq d$, where $t = 1 - T/T_c$ denotes the reduced temperature. In the materials considered here, ξ_{c0}^{φ} is of the order of the lattice constant c so that, for our films, $\xi_{c0}^{\varphi}/d \approx c/d \ll 1$ and hence $T_{KT}(d) \approx T_c$. Moreover, the temperature interval Δt, where, in the bulk, critical fluctuations dominate, is expected to be rather large, *i.e.* $|\Delta t| \approx 0.1$ [9, 10]. Consequently, the condition for observing 3D critical fluctuations, $|\Delta t| > |1 - T_{KT}(d)/T_c|$, appears to be satisfied. The temperature regimes can then be characterized as follows: at low temperatures, where $\xi_c^{\varphi}(T) \leq d_u$ and d_u denotes the thickness of the thinnest unit that is still superconducting, the film exhibits quasi-2D behaviour and resembles a stack of nearly independent layers of thickness d_u. With increasing temperature, $\xi_c^{\varphi}(T)$ will exceed d_u and 3D fluctuations set in around T_0. Close to the temperature T_*, given by $\xi_c^{\varphi}(T_*) \approx d$, the system feels its reduced dimensionality (finite film thickness) and undergoes a KT transition at $T_{KT}(d)$. Nevertheless, if the temperature range $|\Delta t|$, where the 3D critical fluctuations dominate, satisfies the aforementioned condition, $|\Delta t| > |1 - T_{KT}(d)/T_c|$, 3D-$XY$ critical behaviour can be observed. In this view, the measured temperature dependence of L_k is expected to uncover these regimes and to provide a direct estimate of ξ_{c0}^{φ}.

The films used in this study were grown on (001) $SrTiO_3$ substrates using sequential molecular-beam epitaxy (MBE) deposition. Good crystallographic structures with a c-axis single phase were obtained [12], [13]. The width of the resistive transition taken from the midpoint value is found to be nearly independent of x and varies between 2 to 3 K. Accordingly, there is no evidence of a dramatic disorder-induced broadening of the transition. Let us also point out that the microstructure does not vary significantly as a function of doping. The reduced values of T_c in our thin films are consistent with those found in previous studies [14], [15], revealing a substantial reduction of T_c for a nominal thickness of less than 1000 Å. This reduction has been attributed to substrate-induced stress [14], [16]. For further details on the growth technique and film characterization we refer to [12].

In fig. 1, we depict some measurements of the temperature dependence of $L_k(t)$ for an underdoped, an optimally doped, and an overdoped film having a nominal thickness of $d =$ 52 nm. In the intermediate regime ($\Delta t = t_0 - t_*$), $L_k(t)$ is expected to exhibit 3D-XY critical behaviour, namely

$$L_k(t) = L_{k\,0} t^{-\nu} \tag{1}$$

with $\nu \approx 2/3$, whereas for larger t values a crossover to 2D-XY mean-field behaviour with $\nu \approx 1$ is expected to occur. This crossover is clearly seen in fig. 1, where the solid lines represent fits with $\nu \approx 2/3$, as required for 3D-XY critical behaviour, and the dashed lines with $\nu \approx 1$. The parameters T_c and L_{k0} are fit parameters. Thus, around the temperature

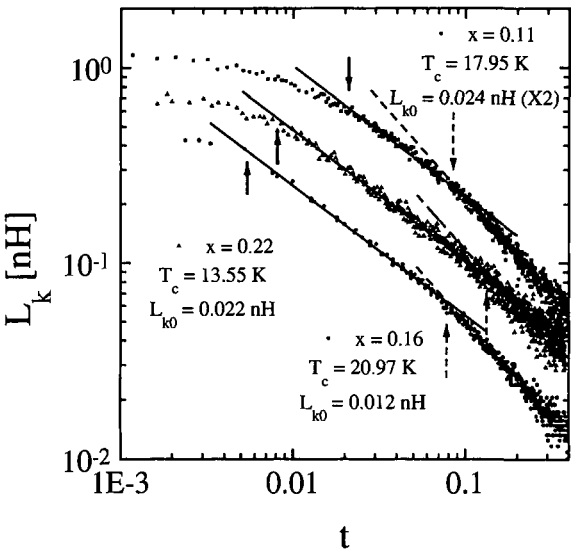

Fig. 1. – Kinetic inductance $L_k(t)$ *vs.* $t = 1 - T/T_c$ for $La_{2-x}Sr_xCuO_4$ films of thickness $d = 52$ nm: $x = 0.11$ (■), $x = 0.16$ (•) and $x = 0.22$ (▲). The solid lines correspond to the slope $v = 2/3$ and the dashed line to $v = 1$. The solid arrows mark the reduced temperature t_* where finite-size effects set in and the dashed arrows locate the temperature t_0 where the crossover from 3D- to 2D-mean-field behaviour occurs. The data for $x = 0.11$ have been scaled by a factor of 2.

t_0 marked by the dashed arrows, the system is seen to cross over from the 2D mean-field to the 3D fluctuation regime. In the latter, the perpendicular real-space phase correlation length grows according to $\xi_c^{\varphi}(t) = \xi_{c0}^{\varphi} t^{-v}$ down to the temperature t_*, where [17], [18]

$$\xi_c^{\varphi}(t_*) = \xi_{c0}^{\varphi} t_*^{-v} = x_c d\,. \tag{2}$$

At t_*, however, the system feels its reduced dimensionality and, for $t < t_*$, the crossover to the 2D-XY critical point sets in. The parameter $x_c \leq 1$ takes into account that the nominal film thickness d might differ from the effective one due to the reduced order parameter at the boundaries of the layer. Moreover, in real films there are substrate-layer and layer-air interfaces, and superconductivity is supposed to be suppressed in these interface regions. In any case, fig. 1 clearly reveals the existence of a temperature regime, Δt, where 3D-XY critical fluctuations dominate as well as the existence of the two temperatures t_* and t_0, marked by solid and dashed arrows, respectively. Indeed, t_* is characterized by the systematic break from $L_k(t) = L_{k0} t^{-v}$ for small t values, where, due to reduced dimensionality, the crossover to the KT critical point sets in. We fixed t_* in the log-log plot as the intersection of the two lines, the first resulting from 3D-XY critical behaviour and the other from assuming linear behaviour below t_*. In fig. 1, it is also seen that these crossover phenomena occur over the full doping regime considered here. Results of our data analysis are shown in fig. 2, 3, and 4. The doping dependence of the transition temperature T_c is depicted in fig. 2 and closely resembles the bulk behaviour [19]. The x-dependence of L_{k0} shown in fig. 3 is more intriguing, because it is seen to increase in both the under- and overdoped regimes from the value at optimum doping. The results for t_*, related to the amplitude of the perpendicular real-space phase correlation length $\xi_{c0}^{\varphi} = x_c d t_*^{v}$ (eq. (2)), are depicted in fig. 4. In agreement with fig. 1, t_* is seen to increase slightly from its value at optimum doping in the under- and overdoped regimes. In terms of

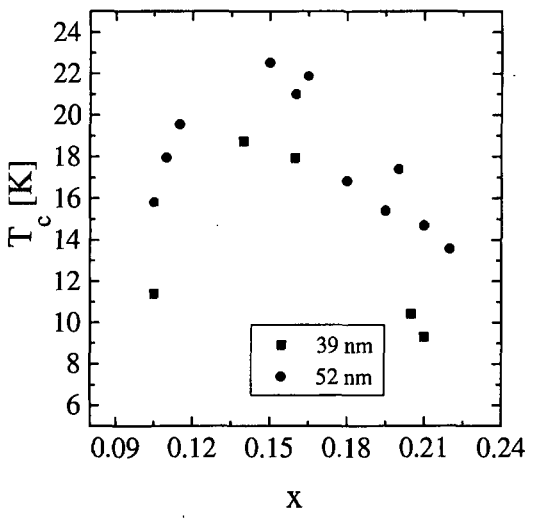

Fig. 2.

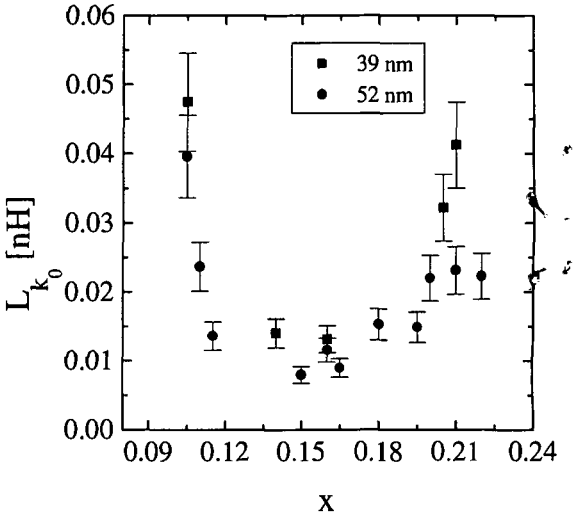

Fig. 3.

Fig. 2. – Transition temperature $T_c(d)$ *vs.* Sr concentration x for $La_{2-x}Sr_xCuO_4$ films of nominal thickness 39 (■) and 52 (•) nm.

Fig. 3. – Doping dependence of the critical amplitude $L_{k0} = \lambda_{ab0}^2/d$. The error bars correspond to an estimated uncertainty of 10%.

the universal 3D-XY critical-point relation [4], [8]

$$k_B T_c = \frac{\Phi_0^2}{16\pi^3} \frac{\xi_{c0}^{\varphi}}{\lambda_{ab0}^2}, \tag{3}$$

connecting T_c with the amplitudes of the penetration depth λ_{ab0} and the phase correlation length ξ_{c0}^{φ}, it becomes clear that the doping dependences of T_c, λ_{ab0} and ξ_{c0}^{φ} are not independent of one another. Indeed, because T_c decreases away from optimum doping (fig. 2), whereas $t_* = (\xi_{c0}^{\varphi}/(x_c d))^{1/\nu}$ increases (fig. 4), $L_{k0} = \lambda_{ab0}^2/d$ (fig. 3) must increase away from optimum doping in order to satisfy the universal relation (3). Thus, the doping dependence of T_c, L_{k0} and t_* shown in fig. 2, 3, and 4 and derived from the measured $L_k(t)$ and finite-size scaling (eq. (2)) are consistent with 3D-XY critical behaviour along the phase transition line $T_c(x)$.

To provide a more quantitative and self-consistent test of our data analysis, we note that the universal relation (3) and the finite-size expression (2) also imply that

$$x_c = k_B T_c \frac{16\pi^3}{\Phi_0^2} \frac{L_{k0}}{t_*^{\nu}}. \tag{4}$$

Full consistency with 3D-XY behaviour requires that x_c be of the order of unity, provided that the films are of good quality. From our data, involving five samples of 39 nm thickness and eleven of 52 nm, we obtain a mean value of $x_c \cong 0.89$ and a deviation of 0.13. This is remarkably consistent with the 3D-XY critical point. Then, since $\lambda_{ab0}^2 = L_{k0} d$, the universal relation (3) can be used to express the perpendicular real-space phase correlation length ξ_{c0}^{φ} in terms of experimentally accessible quantities, namely

$$\xi_{c0}^{\varphi} = k_B T_c \frac{16\pi^3}{\Phi_0^2} L_{k0} d. \tag{5}$$

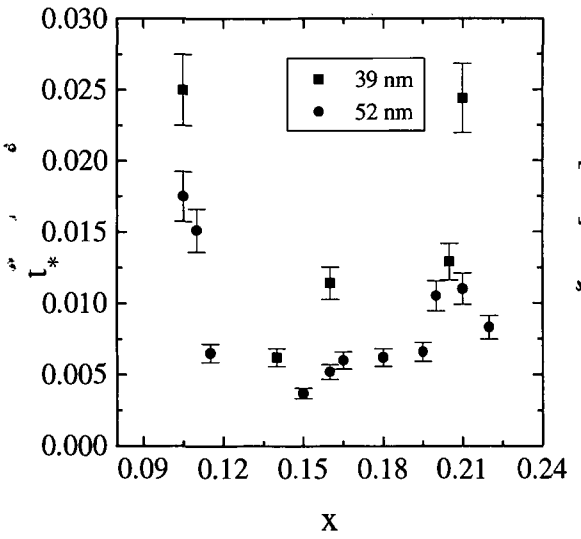

Fig. 4.

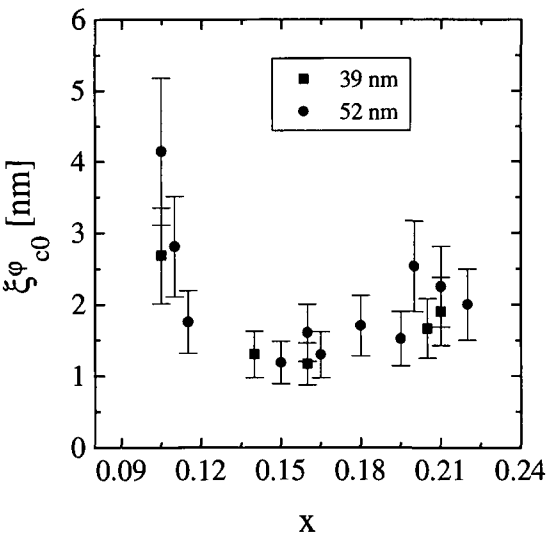

Fig. 5.

Fig. 4. – Temperature t_* as a function of doping derived from finite-size scaling. The error bars correspond to an estimated uncertainty of 10%.

Fig. 5. – Doping dependence of the perpendicular real-space phase correlation length ξ^{φ}_{c0} derived from eq. (5).

The resulting magnitude and doping dependence of ξ^{φ}_{c0} is shown in fig. 5. To our knowledge, these results represent the first experimental determination of the phase correlation length in cuprate superconductors. In fig. 5, it is seen that in both the under- and overdoped regimes, ξ^{φ}_{c0} is larger than the separation of two copper oxide layers (0.66 nm), suggesting that one copper oxide sheet is not superconducting.

In summary, we have presented self-consistent evidence of 3D-XY critical-point behaviour over a considerable doping range, covering the underdoped, optimally doped and overdoped regimes in terms of finite-size scaling (eq. (2)), the temperature dependence of $L_k(t)$ (eq. (1)) and the universal relation (3). Moreover, we determined the perpendicular real-space correlation length ξ^{φ}_{c0} and have shown that the intriguing doping dependence of the penetration depth is a simple consequence of the universal relation (3), given the doping dependence of the T_c and $\xi^{\varphi}_{c0} = dt^{\nu}_*$.

***

This work was supported by the Swiss National Science Foundation.

REFERENCES

[1] LOBB C. J., *Phys. Rev. B*, **36** (1987) 3930.
[2] KAPITULNIK A. *et al.*, *Phys. Rev. B*, **37** (1988) 537.
[3] FISCHER D. S., FISCHER M. P. and HUSE D. A., *Phys. Rev. B*, **43** (1991) 130.
[4] SCHNEIDER T. and ARIOSA D., *Z. Phys. B*, **89** (1992) 267.
[5] UZUNOV D. I., *Theory of Critical Phenomena* (World Scientific, Singapore) 1993.
[6] KOZLOWSKI A. *et al.*, *Physica C*, **184** (1991) 113.

[7] OVEREND N. *et al.*, *Phys. Rev. Lett.*, **72** (1994) 3238.
[8] SCHNEIDER T. and KELLER H., *Int. J. Mod. Phys. B*, **8** (1993) 487.
[9] ZECH D., private communication.
[10] KAMAL S., *Phys. Rev. Lett.*, **73** (1994) 1845.
[11] JEANNERET B. *et al.*, *Appl. Phys. Lett.*, **55** (1989) 2336.
[12] JACCARD Y. *et al.*, *Proceedings of the SPIE Conference on Oxide Superconductors and Nanoengineering, SPIE*, **2158** (1994) 200.
[13] WILLIAMS E. J. *et al.*, *EMAG'93, Liverpool, Inst. Phys. Conf. Ser.* No. 138 (1993), p. 329, section 7.
[14] KAO H. L. *et al.*, *Appl. Phys. Lett.*, **59** (1991) 2748.
[15] YI G.-C. *et al.*, *Physica C*, **194** (1992) 293.
[16] WILLIAMS E. J. *et al.*, *Proceedings of Microscopy & Microanalysis*, edited by G. W. BAILEY *et al.* (Jones & Begell Publishing, New York, N.Y.) 1995, p. 382.
[17] BARBER M. N., in *Phase Transitions and Critical Phenomena*, edited by C. DOMB and J. L. LEBOWITZ, Vol. **8** (Academic Press, New York, N.Y.) 1983, p. 143.
[18] SCHNEIDER T. and SCHMIDT A., *J. Phys. Soc. Jpn.*, **61** (1992) 2169.
[19] TALLON J. L. and FLOWERS N. E., *Physica C*, **204** (1993) 237.

Variation of the in-plane penetration depth λ_{ab} as a function of doping in $La_{2-x}Sr_xCuO_{4\pm\delta}$ thin films on $SrTiO_3$: Implications for the overdoped state

J.-P. Locquet*
IBM Research Division, Zurich Research Laboratory, 8803 Rüschlikon, Switzerland

Y. Jaccard
IBM Research Division, Zurich Research Laboratory, 8803 Rüschlikon, Switzerland and Institut de Physique, Université de Neuchâtel, 2000 Neuchâtel, Switzerland

A. Cretton and E. J. Williams
IBM Research Division, Zurich Research Laboratory, 8803 Rüschlikon, Switzerland and Département de Physique de la Matiére Condensée, Université de Genève, 1211 Genève, Switzerland

F. Arrouy
IBM Research Division, Zurich Research Laboratory, 8803 Rüschlikon, Switzerland and Institut of Inorganic Chemistry, University of Zurich, 8057 Zurich, Switzerland

E. Mächler and T. Schneider
IBM Research Division, Zurich Research Laboratory, 8803 Rüschlikon, Switzerland

Ø. Fischer
Département de Physique de la Matière Condensée, Université de Genève, 1211 Genève, Switzerland

P. Martinoli
Institut de Physique, Université de Neuchâtel, 2000 Neuchâtel, Switzerland

(Received 2 April 1996)

Normal-state properties, such as the resistivity ρ_{ab} and the Hall coefficient R_H, structural properties, such as the c axis and in-plane lattice parameters, and superconductive properties, such as the critical temperature T_c, the penetration depth λ_{ab}, and the thermal activation energy for flux flow ΔU, are reported for c-axis $La_{2-x}Sr_xCuO_{4\pm\delta}$ films. These parameters have been measured as a function of doping in the range from heavily underdoped to heavily overdoped. The structural data indicate a 0.3% compression of the c-axis parameter and a corresponding 0.3% expansion of the in-plane lattice parameters as compared to bulk values, which explains the overall reduced critical temperature of these thin films. As the dopant content is increased, maximum values for T_c, ΔU, and λ_{ab}^{-1} are observed close to optimum doping, while R_H and ρ_{ab} decrease monotonically. [S0163-1829(96)06733-1]

I. INTRODUCTION

It is of fundamental importance to establish the doping (x) dependence of the superconducting properties in cuprate superconductors. Of particular relevance are the phase-transition line $T_c(x)$, which distinguishes the normal from the superconducting state, and the penetration depth $\lambda(x)$. Indeed a maximum T_c is observed for "optimum" doping, with a decrease in both the underdoped and overdoped regimes. The penetration depth λ characterizes the appearance of the Meissner state, and its "true" doping dependence is currently a topic of considerable debate.[1–4] On the other hand, from a phase-transition point of view, an analysis of thermal fluctuations points to three-dimensional (3D) xy critical behavior, which leads to a relation between the specific-heat singularity, λ and T_c, and predicts an increase of λ in the overdoped regime, *independent of any microscopic mechanism of superconductivity*.[5] Recent work on overdoped Tl compounds[1,2] and overdoped $YBa_2Cu_3O_7$ "123" compounds[6] appears to confirm these predictions.

In this paper we report careful measurements of various properties on c-axis $La_{2-x}Sr_xCuO_4$ ("214") thin films, covering the doping regime from heavily underdoped to heavily overdoped. Particular attention was given to the preparation of *high-quality, homogeneous films*. First, the normal-state properties, such as the Hall coefficient R_H and the in-plane resistivity ρ_{ab}, are obtained as a function of doping; they allow an estimate of the mean free path l. Second, the evolution of the structural properties is reported as a function of doping and thickness. Then the thermal activation energy for flux flow, ΔU — related to λ — is derived from $\rho_{ab}(T)$ measurements in a magnetic field close to T_c. Finally, the in-plane penetration depth λ_{ab} is obtained directly from the kinetic inductance L_K for the same samples. About 20 samples have been characterized, and this work represents the most complete study of the behavior of λ from the heavily underdoped to the heavily overdoped regime to date.

The original Sr-doped La_2CuO_4 compound[7] is an attrac-

tive material for such a study, as it supports "bulk" and homogeneous superconductivity over a large range of doping as recently demonstrated.[8,9] The preparation of "bulk" homogeneous "214" samples is tedious (particularly in the overdoped regime), owing to the very slow Sr incorporation into the easily formed undoped 214 lattice during solid-state sintering at the standard temperatures (more than 100 h are necessary for sintering at 900 °C).[9] This effect and the resulting "chemical phase separation" could well explain Uemura's early results[3] as well as the claims that superconductivity is restricted to a narrow composition range.[10,11] From a sample-preparation point of view, the thin-film growth process is ideal for avoiding the occurrence of chemical phase separation. The growth process is mostly 2D, as films with large and atomically flat surfaces (μm size) can easily be obtained.[12] This indicates that the surface diffusion coefficients are certainly large enough to ensure a homogeneous Sr distribution. The films used here were grown on $SrTiO_3$ using sequential molecular-beam deposition; the deposition details and the overall structural properties of the films have been published elsewhere.[12,13] Briefly, x-ray diffraction, atomic force microscopy, and transmission electron microscopy (TEM) revealed single-phase and c-axis single-crystal films with a surface roughness of about one unit cell (over 1 μm^2) and a microstructure that is essentially free of the usual defects observed in high-T_c cuprate films, such as secondary phase inclusions, a-axis inclusions, grain and/or twin boundaries. Strong chemical inhomogeneity, such as that induced by large-scale Sr clustering, can be observed using TEM.[13] However during the TEM investigations of the films, no evidence of such behavior was found in the entire doping range studied.

II. NORMAL-STATE PROPERTIES

The normal-state properties ρ^{-1} and R_H^{-1} obtained at 100 K using standard four-point and Hall-effect measurements are summarized in Fig. 1 as a function of doping. For both quantities a *monotonic increase* is observed with increasing Sr content. They are in *excellent agreement* with literature data of other thin films on $SrTiO_3$ having a comparable thickness, although single crystals and thicker films show reduced resistivities ($\simeq$20–30 %).[14–17] Higher resistivity values are typically taken as evidence of poor sample quality. On the other hand, the resistance ratio ($\rho_{300\ K}/\rho_{50\ K}$) is also a good indicator for the quality of the thin films, and values between 3.3 and 3.5 were obtained for the optimally doped films. These values are as good as or better than those cited for the best films or single crystals reported so far, indicating a similar sample quality.[17] This apparent contradiction originates from a residual in-plane tensile stress, which expands the in-plane lattice constants and increases the resistivity to $\simeq$20–30 %. A quantitative argumentation is given below. We used the published R_H^{-1} values as a calibration curve to correct the experimental uncertainty ($\simeq$10%) in the Sr content of our films.

Models must be used to relate ρ^{-1} and R_H^{-1} to the carrier density n, and only the simplest ones predict a direct proportionality, $\rho^{-1} \propto n$ and $R_H^{-1} \propto n$. Although more elaborate models could modify these predictions, we expect that ρ^{-1} and R_H^{-1} increase with n. Therefore our data suggest that the carrier density increases with Sr doping. Further evidence of this comes from normal-state measurements of the Cu spin-lattice-relaxation rate, the magnetic shift and the spin susceptibility obtained from nuclear magnetic resonance (NMR) experiments on this compound[18] as well as on overdoped $YBa_2Cu_3O_7$ (Ref. 19) and $Tl_2Ba_2CuO_6$.[20,21] These *independent* measurements clearly suggest that an increase in the Sr content indeed increases n.

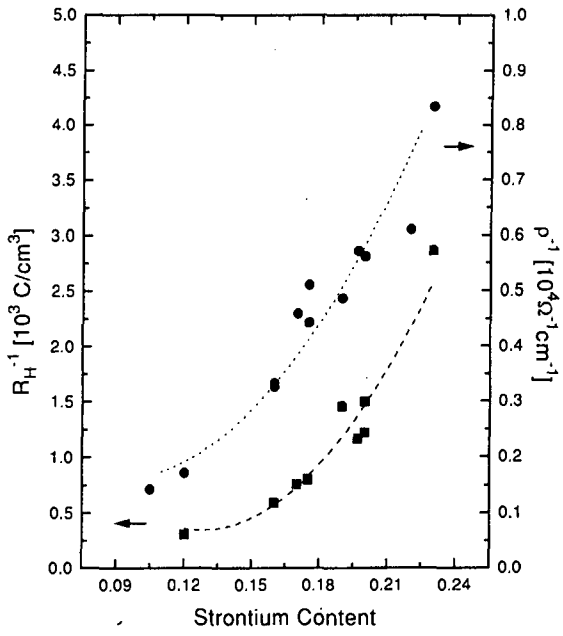

FIG. 1. Inverse resistivity (●) and inverse Hall coefficient (■) at 100 K versus Sr concentration.

III. STRUCTURAL PROPERTIES

While the normal-state properties are in excellent agreement with literature values, there is a significant difference between the lattice parameters of 214 thin films on $SrTiO_3$ and those of the bulk 214. From θ–2θ x-ray-diffraction experiments, the value of the c-axis lattice parameter can be derived and is shown in Fig. 2 as a function of Sr content for our thin and thick films as well as for bulk samples.[22] These data are in very good agreement with those recently reported for laser-ablated 214 thin films on $SrTiO_3$.[23] Although there is an experimental error ($\pm$0.01 Å) in the determination of the c-axis lattice parameter for the thin films, a comparison between the data of films and bulk material indicates an average difference of $\simeq$0.045 Å, i.e., a contraction of about 0.35%. To compress the bulk 214 lattice to such an extent along the c axis, a pressure of 1.6–2.2 GPa (depending on Sr doping) would be necessary under *hydrostatic* conditions.[24]

There are two possible origins for this difference in lattice parameters. First, it is well documented that an oxygen deficiency in the 214 lattice gives rise to a reduced c-axis lattice parameter. This possibility can be excluded, as the samples are cooled under a flow of atomic oxygen that is sufficiently powerful to fill even some interstitial oxygen sites and that can induce superconductivity at 32 K in 214 thin films prepared without Sr, ($La_2CuO_{4+\delta}$).[32] In addition, a post-annealing of these films in an oxygen atmosphere at

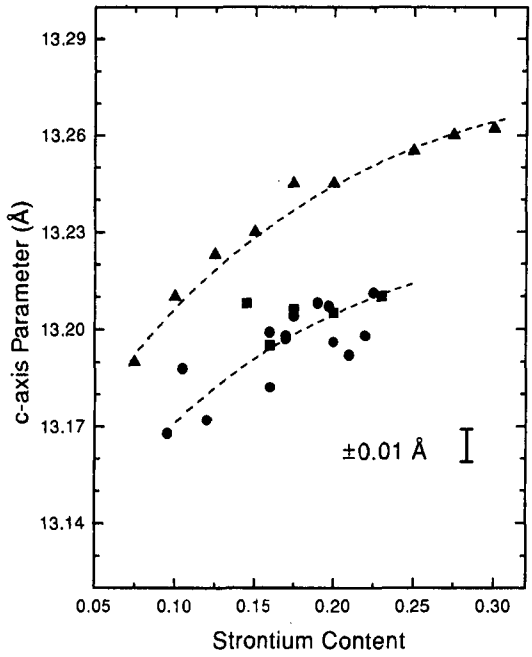

FIG. 2. Evolution of the c-axis lattice parameter versus Sr concentration for thick (■) and thin (●) films as well as for bulk samples (▲).

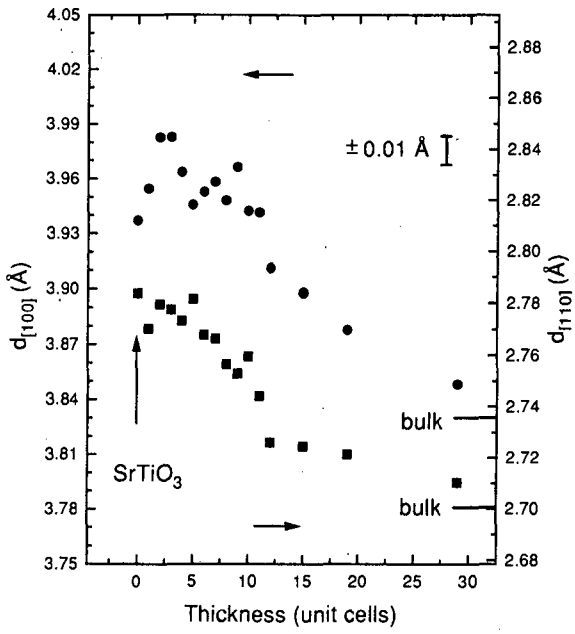

FIG. 3. Evolution of the in-plane $d_{[100]}$ (●) and $d_{[110]}$ (■) lattice parameters as a function of thickness for an undoped 214 film.

700 °C for 24 h does not significantly change the lattice parameters. The second possibility is related to the in-plane lattice parameter difference between $SrTiO_3$ (3.9 Å) and 214 (3.8 Å). The 2.5% larger in-plane lattice parameter of the substrate could be partially responsible for the film in-plane lattice parameter extension, which would induce a shorter c-axis lattice parameter. During thin film growth such a large discrepancy between lattice parameters is usually accommodated by the appearance of misfit dislocations (for thicknesses larger than the critical thickness). For our 214 thin films, we have shown[13] that a regular network of misfit dislocations exists that accommodates "most" of the lattice misfit.

To find out whether the lattice misfit is completely accommodated by the creation of misfit dislocations, we have performed a detailed analysis of *in-situ* reflection high-energy electron diffraction (RHEED) spectra recorded during the deposition of an undoped 214 film on $SrTiO_3$ at 750 °C. The RHEED images of the film present a series of long streaks at regular spacings, characteristic of two-dimensional growth.[12] Line scans taken across such spectra show a series of peaks that have been fitted using the Phearson VII peak profile. From the peak positions the in-plane lattice parameter can be estimated *in principle* with an accuracy of $\simeq 0.01$ Å. However to obtain an accurate absolute value the precise geometrical diffraction conditions must be known. Minute geometrical changes of the sample manipulator during a temperature ramp currently prevent a measurement of the lattice parameters as a function of the temperature. Hence such a precision can only be maintained for a comparison under identical conditions (such as during growth). A more detailed report of this method and the analysis of the *in-situ* RHEED data is in preparation.[25]

To calibrate the vertical axis of Fig. 3 precisely we have used the lattice parameter of the substrate but extrapolated to 750 °C by using literature values of the thermal-expansion coefficients (α) of $SrTiO_3$ and 214. For $SrTiO_3$, $\alpha \simeq 11\times10^{-6}$/K,[26] which gives a $d_{[100]}$ spacing of 3.937 Å. The only data we found regarding the thermal expansion of undoped 214 at temperatures much above the orthorhombic–tetragonal phase-transition temperature are given in Ref. 27, namely, $\alpha \simeq 8.5\times10^{-6}$/K and a $d_{[100]}$ spacing of 3.826 Å.

The evolution of the [100] and [110] lattice parameters is shown in Fig. 3 as a function of the number of unit cells deposited. The extrapolated bulk 214 values (3.826 and 2.703 Å, respectively) are indicated by the short lines on the right-hand axis. For the first unit cells (up to $\simeq$100 Å), the in-plane lattice parameter is very close to that of the substrate. For larger thicknesses — as the creation of misfit dislocations sets in — a decrease of the lattice parameters is observed, but even at the maximum thickness studied here, there is no saturation. In addition, the thin-film values are still larger than the bulk lattice parameters, suggesting that the strain is not yet completely relieved. This remaining difference — averaged over the two data sets — corresponds to an in-plane lattice expansion of about 0.4%. Owing to the faster thermal contraction of the substrate as the sample cools after deposition, this mismatch might be reduced at room temperature. The misfit dislocations have been observed,[13] and their strain fields distort the film at the film/substrate interface over a typical distance of 2–6 unit cells, occasionally even up to 12 unit cells. Nevertheless careful measurement of the misfit-dislocation spacings[28] of Sr-doped 214 films has recently confirmed that strain remains present in the film.

Within the resolution ($\simeq$0.01 Å) of the available instruments (x-ray diffraction, RHEED, and TEM), all thin films discussed here have a tetragonal structure. Even thin films of the undoped 214 compound — which has the largest orthorhombic distortion ($b-a \simeq 0.05$ Å) in bulk samples — show no deviation from the tetragonal symmetry. It is known that

the undoped orthorhombic 214 lattice can be transformed into a tetragonal lattice by the application of *hydrostatic* pressure of about 4 GPa.[29]

The above experimental data (the room-temperature c-axis lattice parameters, the high-temperature *in-plane* lattice parameters, and the absence of an orthorhombic distortion) unambiguously suggest that the thin films on $SrTiO_3$ are under tension. Unfortunately, these data were gathered under widely different experimental conditions, and with insufficient precision to allow a fully quantitative stress analysis. Qualitatively, however, the *cause* of this stress is an increased *in-plane* lattice parameter with a reduced c-axis lattice parameter as a *consequence*. Experimentally, an identical situation cannot be realized using high-pressure methods. In a uniaxial pressure experiment, cause and consequence are interchanged compared to our case, but similar changes in lattice parameters should be observed. Since no literature data are available regarding the evolution of the lattice parameters under uniaxial pressure, estimates from hydrostatic or quasihydrostatic experiments are used. The above lattice parameters show that the films are under tension, in a state that is qualitatively equivalent to the application of a *pseudouniaxial* pressure of the order of 2–3 GPa along the c axis.

As described by Goodenough and Manthiram[30] for the 214 compounds the La_2O_2 sheets are under tension in the K_2NiF_4 structure, because the eight La-O distances measured (three La-O distances $\simeq$2.52 Å, five La-O distances $\simeq$2.714 Å) are close to or larger than the sum of the ionic radii: 2.55 Å. However, the cohesion of the structure is ensured by the very short apical La-O bond ($\simeq$2.35 Å). If the a and b lattice parameters increase — as is the case in our films — the lateral La-O distances should also increase, which therefore induces even more lateral tension in the La_2O_2 sheets. In order to compensate such a stress, the apical La-O distances must decrease, corresponding to a decrease of the c axis in our thin films.

In the following paragraph we compare the normal-state properties of the films with those of bulk compounds under pressure. Unfortunately only few uniaxial-pressure measurements on the 214 compound exist. Therefore we make the reasonable assumption that the observed in-plane film properties are affected by the in-plane epitaxial tensile strain (i.e., a negative pressure) to a similar *magnitude* as is found under hydrostatic (positive) pressure for bulk compounds, but with *opposite sign.*

For the 214 system, it has been shown by Tanahashi *et al.*[31] that hydrostatic pressure has only a small effect (a few %/GPa) on the Hall coefficient over the entire doping range (0.08–0.24), which is in contrast to the sizable dependences found in the other hole-doped superconductors.[24] We are unaware of any uniaxial pressure Hall effect measurements, but a change of $\simeq$10% in Hall coefficient is reasonable. For instance, those films that have a maximum critical temperature for a given thickness, show a Hall coefficient within 10% of the corresponding bulk value, suggesting that this effect is indeed small. Since we calibrated the actual Sr content in the films using the Hall coefficient of bulk samples, an uncertainty in the Sr content of our films is also expected. The changes in the resistivity under hydrostatic conditions are larger ($\leq$10%/GPa) (Ref. 24) for this compound, and again, to our knowledge, no uniaxial measurements are available. However, since the in-plane lattice parameters increase, the in-plane resistivity (ρ_{ab}) must increase accordingly, while the out-of plane resistivity (ρ_c) and the anisotropy (ρ_c/ρ_{ab}) must decrease. Further proof of this mechanism comes from the growth of 214 thin films on $SrLaAlO_4$ substrates, where the lattice mismatch is much smaller and in the opposite direction. In this case, the in-plane and c-axis lattice parameters are very close to the bulk values.[25] The resistivity of these thin films is indeed smaller ($\simeq$20–30%), in excellent agreement with those of thick films and single crystals and a high critical temperatures can be reached (38 K).

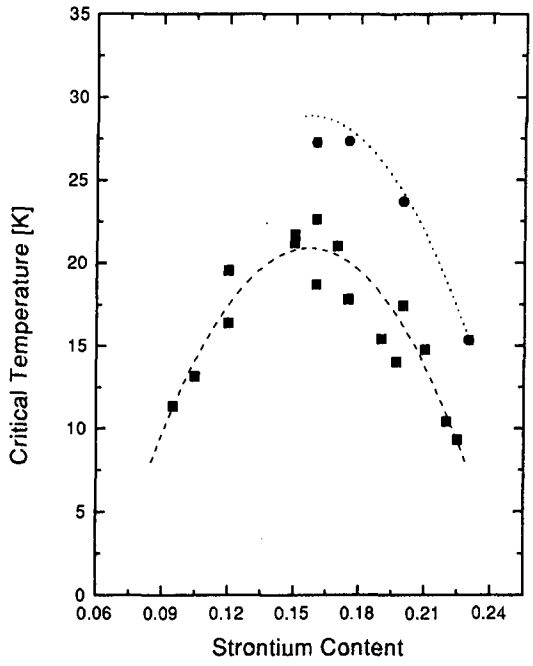

FIG. 4. The critical temperature as a function of Sr concentration for thin (■) and thick (●) films.

IV. CRITICAL TEMPERATURE

The critical temperature (T_c) versus x was measured both resistively and inductively, and is shown in Fig. 4 for both thin (39, 50, and 65 nm) and thick (200 nm) films prepared under identical conditions. Typical transitions widths — in both types of measurements — are 2–3 K, independent of the amount of doping. There is no evidence for a composition-dependent zero-field broadening of the transition. The maximum critical temperature observed, at optimum doping ($x=0.16$) for the thickest films, is about 28 K; away from optimal doping, the critical temperature decreases. These data also confirm the well-known but not yet understood trend that the critical temperature of thin 214 films grown on $SrTiO_3$ strongly depends on the film thickness,[14,17] a T_c above 30 K being observed only for very large thicknesses.

Different structural phases with a different T_c occur in the 214 system as the structural details, such as the octahedral tilting angle and the orthorhombicity, are changed.[33] In thin films on a lattice-mismatched substrate, these parameters are

expected to differ from bulk values. The structural study presented here showed the presence of a significant tensile strain, which might explain — at least partially — the reduced critical temperature of these films. To our knowledge only one direct experiment of the uniaxial pressure dependence of the critical temperature is available in the literature: Motoi *et al.*[34] studied this property on grain-aligned 214 composites as a function of Sr doping and found that T_c decreases, at the rate of 3 to 9 K/GPa, under pressure applied along the c axis, depending on the doping level.

Alternatively the uniaxial pressure derivatives of T_c can be obtained by measuring the thermal-expansion anomalies at T_c along the different crystallographic orientations using the Ehrenfest relation. This method, which requires the knowledge of the specific-heat jump at the transition temperature, has been used by several authors,[24,35–37] and estimates of approximately -6 to -7 K/GPa for dT_c/dP_c (for pressure applied along the c axis), 2 K/GPa for dT_c/dP_a, and 5 K/GPa dT_c/dP_b have been reported for optimally doped samples. These data on bulk 214 samples, together with in-plane tensile strains equivalent to an estimated pseudouniaxial pressure of the order of 2 GPa, can easily explain the drastic reduction of the critical temperature in thin films to values around 20 K. A more quantitative analysis would require measurements of the pressure dependence of the critical temperature of both a- and c-axis 214 thin films as was done by Bud'ko *et al.*[38] for 123.

For thicker films more strain is relieved (although this is not clearly visible from the data in Fig. 2). The critical temperature is indeed higher, but the general trend of T_c versus x is the same for both thicknesses (see Fig. 4). Indeed, it is well known that applying pressure to this high-T_c cuprate changes the *absolute values* of the critical temperature but does not affect the *general trend* of the superconducting properties (for instance, the maximum of $T_c(x)$ still occurs for $x \simeq 0.16$). Applying a high-pressure oxygen treatment to such thin films can restore the bulk critical temperatures.[39] We did not perform such a treatment, as it introduces yet another process variable and as it can change the carrier density if additional oxygen is incorporated.

V. COMPLEX IMPEDANCE MEASUREMENTS

To determine λ, several methods have been used, such as muon spin resonance (μSR) measurements,[3] "mixed-state" magnetization isotherms[8,40] [i.e., $M(H)$ in the reversible regime], and microwave experiments.[41] Here we derive λ_{ab} from a two-coil mutual inductance measurement.[42] This technique allows the complex sheet impedance $Z_\square = R_\square + i\omega L_\square$ to be extracted from the measured real and imaginary parts of the signal using a numerical inversion procedure. In zero field, $L_\square$ is the sheet kinetic inductance L_K, which is related to the penetration depth λ_{ab} by $L_K = \mu_0 \lambda_{ab}^2/d$, with μ_0 the vacuum permittivity and d the film thickness. On the other hand, $R_\square = \rho_{ab}/d$ is related to dissipation resulting from vortex motion.

A. Activation energy

Close to T_c and in a magnetic field parallel to the c axis, we find that $\ln\rho_{ab}$, as inferred from resistive and inductive measurements, varies linearly with $1/T$, implying thermally activated vortex motion over a pinning barrier. The activation energies $\Delta U(T=0)$ derived from the inductively measured $\rho_{ab}(T)$ curves at $H=0.4$ T are presented in Fig. 5 as a function of x for different film thicknesses. These data are very different from those reported in the literature,[14] where a large field broadening was observed in the underdoped regime, but not in the overdoped regime. We want to point out that the field used here (0.4 T) is much smaller and that the activation energy is obtained from ρ_{ab} values that are very close to the onset of resistance, in the resistivity range between 10^{-3} and $10^{-6}\mu\Omega$ cm, i.e., five to eight decades below $\rho_{50\ \mathrm{K}}$ (see figures in Ref. 12). Hence these data cannot easily be related to those extracted from the broadening of the resistive transition in the 100 $\mu\Omega$ cm range and the doping dependence reported.[14]

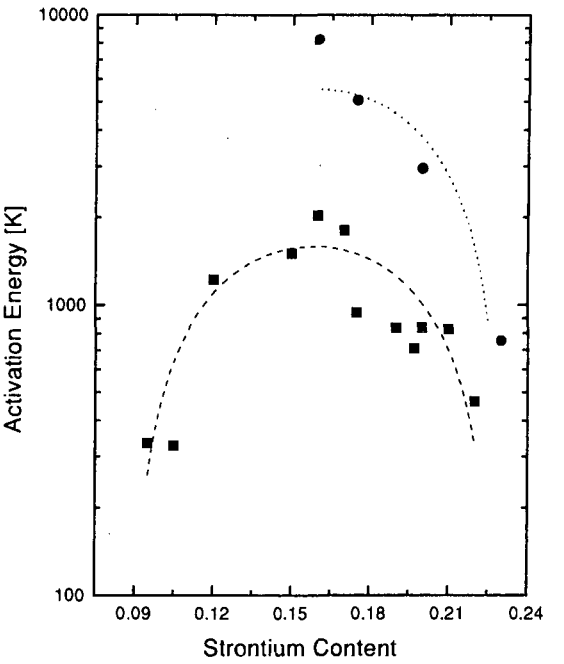

FIG. 5. The activation energy for flux flow $\Delta U/k_B$ (expressed in temperature units) as a function of the Sr concentration for thin (■) and thick (●) films.

In Fig. 5 ΔU reaches a maximum the height of which depends on the film thickness for optimum doping and decreases as one deviates from it. It is generally expected that ΔU is proportional to $1/\lambda^2$. For instance, Feigel'man *et al.*[43] propose that the activation energy of a dislocation pair in the 2D collective-pinning model behaves as $\Delta U = (\Phi_0^2 d/16\pi^2\mu_0\lambda_0^2)\ln(a_0/\xi_0)$,[44] where a_0 is the flux-line lattice spacing. Since $a_0/\xi_0 \gg 1$ at the field of interest in our studies, the logarithmic term is a slowly varying function of x, so that $\Delta U(x)$ is essentially proportional to $\lambda^{-2}(x)$. Another relation was proposed by Blatter *et al.*[45] for the case of a single vortex along the c axis of a 3D superconductor containing randomly distributed, weak pinning centers: $\Delta U = \Phi_0^2\xi_0\delta^{1/3}\varepsilon^{2/3}/8\pi^2\mu_0\lambda_0^2$, where δ is a disorder parameter and ε^2 the mass anisotropy. Although ε is strongly doping dependent in the underdoped case, it becomes almost constant in the overdoped regime,[8] and therefore $\Delta U(x) \propto \lambda^{-2}(x)$. Thus the conclusion emerging from the data in

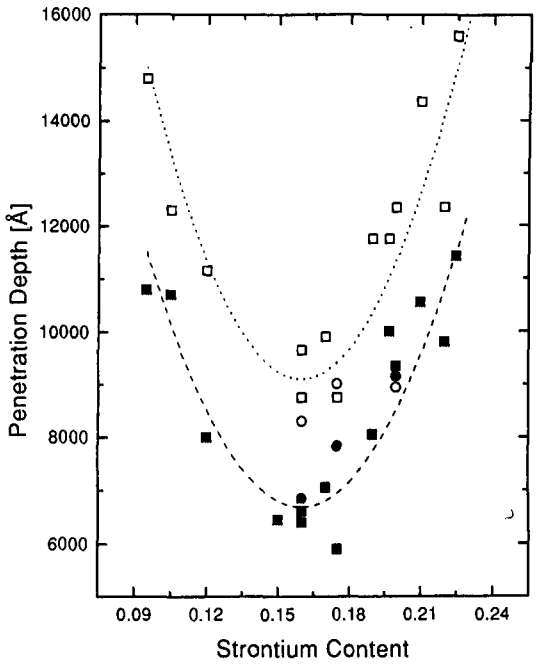

FIG. 6. The penetration depth λ_{ab} as a function of Sr concentration derived using the critical fluctuations close to T_c (■): thin and ●: thick films) and using a two-fluid extrapolation to 0 K (□: thin and ○: thick films).

Fig. 5 is that $\lambda(x)$ is *nonmonotonic* in x with a minimum value at optimum doping. Stronger pinning, as suggested in Ref. 8, and/or a larger disorder δ cannot explain the data in the overdoped regime.

B. Penetration depth

Additional and even stronger evidence of the nonmonotonic $\lambda^{-2}(x)$ with Sr doping is provided by direct measurements of λ_{ab} using the mutual-inductance technique. The temperature dependence of $\lambda_{ab}(T)$ has already been published.[12] Except for the temperature regime close to T_c (where critical fluctuations play an important role), the temperature dependence can be fitted reasonably well with a two-fluid relation $\lambda/\lambda_0(T)=[1-(t)^4]^{-1/2}$, $(t=T/T_c)$, allowing the extrapolation of λ to $T\rightarrow 0$ K. Figure 6 shows the extrapolated $\lambda(0)$ (open symbols) as a function of doping. Fitting the same data with a BCS-type relation reduces the absolute values of $\lambda(0)$ by $\sqrt{2}$, but does not change the doping dependence. Note that in the present context the detailed temperature dependence is unimportant, as the experimental data at a specific value of t are already sufficient to illustrate our point.[12] For instance, an alternative derivation of λ is provided by an analysis of the data close to T_c. In this region 3D fluctuations lead to a $\lambda(T)/\lambda_0=[1-t]^{-1/3}$ dependence,[5,12] and values of λ_0 have been included in Fig. 6 (filled symbols). It is expected that $\lambda_0\leq\lambda(0)$, as observed experimentally, but regardless of the values used, a *nonmonotonic* behavior of $\lambda(x)$ with a minimum close to optimum doping is obtained. The values for thick films confirm this observation and have also been included (●).

We do not place too much emphasis on the absolute values of the penetration depths obtained, as several experimental details render a comparison with bulk samples [where $\lambda_{ab}(0)\simeq 3000$ Å at optimum doping[40]] difficult. First, a simple relation between T_c and λ_0 has been observed experimentally, namely *the Uemura plot*[3] that partially explains the large values of the penetration depth observed here: the values of $\lambda_0\simeq 6000$ Å are simply due to the lower T_c between 20 and 30 K.[3,4,8] Indeed, this experimental correlation yields a relation between T_c and λ_0 of optimally doped cuprate superconductors: $T_c\propto\lambda_0^{-2}$. Hence, rather than a bulk λ_0 value of $\simeq 3000$ Å, our films would ideally have a λ_0 value of $\simeq 4200$ Å, close to what we actually observe.

Secondly, to deduce λ_0 from the measured L_K, we have used the nominal film thickness. Actually, on account of the presence of strain fields which suppress superconductivity in those portions of the film which are close to the substrate, the effective thickness where superconductivity is established homogeneously might be less than the nominal one, thereby leading to smaller values of λ_0.

Thirdly, the equation[42] used to derive the value of L_K from the inductive measurements is valid for shielding currents extending over very large radii. The lateral dimensions of our thin films (1 cm^2, i.e., only 2–3 times larger than the driving-coil diameter) will certainly affect the shielding efficiency, which might lead to higher values of the penetration depth.

Finally, we have shown that the films are subject to an in-plane *epitaxial tensile strain* that reduces T_c. It is not known to what extent this strain influences the absolute values of the penetration depth or its anisotropy (λ_{ab}/λ_c). In any case, the first argument is certainly valid, and the remaining difference between the bulk and our thin-film values (4200–6000 Å) is probably due a combination of the three other experimental constraints. As the remaining difference is rather small, *the observed behavior is intrinsic and cannot be an artefact due to the sample quality.*

These different experimental constraints are not expected to be a strong function of doping, thus we focus on *the general trend of the data* as a function of Sr content rather than on the absolute values. For instance, when comparing our film data in the underdoped regime to those available for bulk samples,[3,4,8] the same experimental trend can be observed [in both cases $\lambda(0)(x=0.1)/\lambda(0)(x=0.16)\simeq 2$]. In the overdoped regime, values of λ are difficult to obtain for bulk samples.[8] The thin-film data presented here are the first for heavily overdoped 214 samples, and *the excellent agreement between the films and bulk samples in the underdoped regime suggests that the observed nonmonotonic behavior in the overdoped regime is an intrinsic property of this compound.*

VI. DISCUSSION

The results obtained from resistive and inductive measurements indicate that, despite the fact that more carriers are being added to the system, the screening capability of the superconductor is reduced in the overdoped regime. *This is the main result of our paper and is in marked contrast to the simple London prediction* $\lambda_{ab}^{-2}\propto n_s/m^*$. This effect has also been observed in overdoped Tl and 123 compounds.[1,2,6]

A. Dirty limit

Such a behavior could be expected for a superconductor in the dirty limit ($l \ll \xi_0$), and estimates indicate that l must be smaller than $\xi_0/10$ in order to explain the observed upturn. The mean free path in the 214 system has been estimated from resistivity[46] and infrared[47] measurements. From the resistivity measurements a value of $\rho \times l = 3 \times 10^{-10}$ $\Omega\,\mathrm{cm}^2$ has been derived for an optimally doped sample. For the regime of interest (optimally to overdoped), our ρ values — close to T_c — are between 100 and 200 $\mu\Omega$ cm, which gives a mean free path of 300 to 150 Å, respectively. The infrared measurement of a thick, optimally doped 214 film (8200 Å) close to T_c, led to an estimate of $l \simeq 275$ Å a value that is in agreement with the resistivity measurement. From these estimates, it is clear that l is much too large compared to the quoted short coherence length in these cuprates, to explain the observed upturn in λ.

B. 3D xy

The results are consistent with the analysis of thermal fluctuations close to T_c (3D xy critical behavior), which leads to a relation between the specific-heat singularity, λ and T_c.[5] With this relation, λ can be derived from the specific-heat singularity and T_c, $T_c \propto \lambda_0^{-2}$, and an increase of λ in the overdoped regime is predicted, *independent of any microscopic mechanism of superconductivity*. Hence, the 3D xy behavior extends over the entire phase-transition line $T_c(x)$. Recently this consistency, together with a finite-size effect observed in the temperature dependence of λ close to T_c, was used to derive the amplitude of the perpendicular real-space phase correlation length ξ_{c0}^{ϕ} as a function of doping for the same series of samples.[48]

C. n_s/m^*

On a microscopic basis, λ is related to other parameters of the superconducting state, such as the superfluid density n_s (not to be confused with the carrier density) and the effective mass of the carriers m^*: $\lambda^{-2} \propto n_s/m^*$. This raises the question whether the superfluid density n_s or the effective mass m^* is responsible for the increase of λ as doping proceeds beyond the optimum value. Various possibilities have already been suggested.[1,40] To go beyond these arguments, the question to be addressed is whether these additional carriers introduced in the system beyond optimum doping all contribute to the superfluid, i.e., whether $n_s \rightarrow n$ at zero temperature and/or whether microscopic phenomena (on length scales smaller than λ), such as a *chemical* or an *electronic phase separation*,[49] could actually lower n_s. An analysis of the optical conductivity,[50] the ^{63}Cu relaxation rate, the ^{63}Cu Knight shift,[51] and of the specific heat[52] suggests that the added carriers in the overdoped regime only partially condense into pairs.

VII. CONCLUSIONS

We have shown that the epitaxial driving force imposes a residual tension on the 214 thin films grown on $SrTiO_3$. This tension has significant effects on both the normal state and the superconducting properties of these films, mainly by increasing the resistivity and decreasing the critical temperature. Measurements of the penetration depth as a function of doping reveal a nonmonotonic dependence, previously not observed in this compound. After completion of this work, we have been informed that μSR measurements of the doping dependence of λ in bulk 214 compounds[53] are fully consistent with our observations.

ACKNOWLEDGMENTS

The authors wish to thank K. A. Müller, J. G. Bednorz, J.-M. Triscone, D. Ariosa, R. Micnas, J. J. Rodríguez-Núñez, and C. Rossel for stimulating discussions, and the Swiss National Science Foundation for financial support through the PNR30 program. M. Pedersen, K. Kitazawa, and S. Ushida have contributed considerably towards the understanding of the behavior of overdoped compounds. We also thank I. Mangelschots and K. Ishida for relating the NMR data to our results.

*Corresponding author, electronic address: loc@zurich.ibm.com

[1] Y. J. Uemura *et al.*, Nature (London) **364**, 605 (1993).
[2] C. Niedermeier *et al.* (unpublished); C. Niedermeier *et al.*, Phys. Rev. Lett. **71**, 1764 (1993).
[3] Y. J. Uemura *et al.*, Phys. Rev. Lett. **62**, 2317 (1989); Phys. Rev. B **38**, 909 (1988).
[4] T. Schibauchi *et al.*, Phys. Rev. Lett. **72**, 2263 (1994).
[5] T. Schneider *et al.*, Physica C **216**, 432 (1993); T. Schneider, Proc. SPIE **2157**, 2 (1994).
[6] C. Bernhard *et al.*, Phys. Rev. B **52**, 10 488 (1995).
[7] J. G. Bednorz and K. A. Müller, Z. Phys. B **64**, 189 (1986).
[8] K. Kitazawa *et al.*, Appl. Supercond. **1**, 567 (1993); T. Nagano *et al.*, Phys. Rev. B **48**, 9689 (1993).
P. G. Radaelli *et al.*, Phys. Rev. B **49**, 4163 (1994).
R. B. Van Dover *et al.*, Phys. Rev. B **35**, 5337 (1987); K. Yoshimura *et al.*, J. Phys. Soc. Jpn. **59**, 3073 (1990).
D. R. Harshman and A. P. Mills, Jr., Phys. Rev. B **45**, 10 684 (1992).
Y. Jaccard *et al.*, Proc. SPIE **2158**, 200 (1994); Physica C **235–240**, 1811 (1994).
[13] E. J. Williams *et al.*, in *Electron Microscopy & Analysis 1993*, edited by A. Craven, IOP Conf. Proc. No. 138 (Institute of Physics and Physical Society, London, 1994), p. 329; E. J. Williams *et al.*, *Proceedings of the 13th Int'l Congress on Electron Microscopy (ICEM13), Paris, France, July 1994*, edited by B. Jouffrey, C. Colliex, J. P. Chevalier, F. Glas, and P. W. Hawkes (Les Editions de Physique, Paris, 1994), Vol. 2A, p. 987.
[14] M. Suzuki, Phys. Rev. B **39**, 2312 (1989); M. Suzuki and M. Hikita, *ibid.* **44**, 249 (1991).
[15] H. Y. Hwang, B. Batlogg, H. Takagi, H. L. Kao, J. Kwo, R. J. Cava, J. J. Krajewski, and W. F. Peck, Jr., Phys. Rev. Lett. **72**, 2636 (1994).
[16] H. Takagi *et al.*, Phys. Rev. Lett. **69**, 2975 (1992).
[17] H. L. Kao *et al.*, Appl. Phys. Lett. **59**, 2748 (1991).
[18] Y.-Q. Song *et al.*, Phys. Rev. Lett. **70**, 3131 (1993).
[19] M. Takigawa *et al.*, Phys. Rev. B **43**, 247 (1991).
[20] K. Fujiwara *et al.*, Physica C **184**, 207 (1991); K. Fujiwara *et al.*, J. Phys. Soc. Jpn. **59**, 3459 (1990).
[21] Y. Itoh *et al.*, J. Phys. Soc. Jpn. **63**, 22 (1994).

[22] H. Takagi *et al.*, Phys. Rev. B **40**, 2254 (1989).
[23] G. Rietveld, M. Glastra, and D. van der Marel, Physica C **241**, 257 (1995).
[24] J. S. Schilling and S. Klotz, in *Physical Properties of High Temperature Superconductors*, Vol. 3, edited by D. M. Ginsberg (World Scientific, London, 1992), p. 59.
[25] J.-P. Locquet *et al.* (unpublished).
[26] H. J. Scheel, Mater Res. Bull. **19**, 26 (1994).
[27] F. Tresse, Ph.D. thesis, University of Bordeaux, France, 1990.
[28] E. J. Williams *et al.*, *Proceedings of Microscopy and Microanalysis*, edited by G. W. Bailey *et al.* (Jones & Begell, New York, 1995), p. 382.
[29] H. Takahashi *et al.*, Phys. Rev. B **50**, 3227 (1994).
[30] J. B. Goodenough and A. Manthiram, J. Solid State Chem. **88**, 115 (1990).
[31] N. Tanahashi *et al.*, Jpn. J. Appl. Phys. Lett. **28**, L762 (1989).
[32] F. Arrouy *et al.*, this issue, Phys. Rev. B **54**, 7512 (1996).
[33] Wu. Ting and K. Fossheim, Phys. Rev. B **48**, 16 751 (1993).
[34] Y. Motoi *et al.*, J. Phys. Soc. Jpn. **60**, 384 (1991).
[35] Y. Maeno *et al.*, in *Advances in Superconductivity VI*, edited by T. Fujita and Y. Shiohara (Springer-Verlag, Tokyo, 1994), p. 103.
[36] C. Meingast *et al.*, Physica C **235-240**, 1313 (1994); F. Gugenberger *et al.*, Phys. Rev. B **49**, 13 137 (1994).
[37] M. Braden *et al.*, Phys. Rev. B **47**, 12 288 (1993).
[38] S. L. Bud'ko *et al.*, Phys. Rev. B **46**, 1257 (1992).
[39] M. Z. Cieplack *et al.*, Appl. Phys. Lett. **65**, 3383 (1994).
[40] Q. Li *et al.*, Phys. Rev. B **47**, 2854 (1993).
[41] S. M. Anlage *et al.*, Appl. Phys. Lett. **54**, 2710 (1989).
[42] B. Jeanneret *et al.*, Appl. Phys. Lett. **55**, 2336 (1989).
[43] M. V. Feigel'man, V. B. Geshkenbein, and A. I. Larkin, Physica C **167**, 177 (1990).
[44] O. Brunner *et al.*, Phys. Rev. Lett. **67**, 1354 (1991).
[45] G. Blatter, M. V. Feigel'man, V. B. Gesyhkenbein, A. I. Larkin, and V. M. Vinokur (unpublished).
[46] M. Gurvitch and A. T. Fiory, Phys. Rev. Lett. **59**, 1337 (1987).
[47] F. Gao *et al.*, Phys. Rev. B **47**, 1036 (1993).
[48] Y. Jaccard *et al.*, Europhys. Lett. **34**, 281 (1996).
[49] K. A. Müller, in *Phase Separation in Cuprate Superconductors*, edited by K. A. Müller and G. Benedek, The Science and Culture Series: Physics, Proceedings of the Int'l School of Solid State Physics – 3rd Workshop, Erice, Italy (World Scientific, Singapore, 1993), and references therein.
[50] S. Uchida, *et al.*, J. Low Temp. Phys. **95**, 109 (1994).
[51] S. Ohsugi, *et al.*, J. Phys. Soc. Jpn. **63**, 700 (1994).
[52] J. W. Loram, *et al.*, Physica C **235-240**, 134 (1994).
[53] H. Keller, *et al.* (private communication).